Electronic Supplementary Material (ESI) for Physical Chemistry Chemical Physics.

Insights into exfoliation of MAX phases from bonding properties of their neutral and charged phases

Mohammad Khazaei,*[1] Ahmad Ranjbar,[1] Keivan Esfarjani,[2] Dimitri Bogdanovski,[3]
Richard Dronskowski,[3] Seiji Yunoki[1,4,5]

[1]Computational Materials Science Research Team,
RIKEN Advanced Institute for Computational Science (AICS), Kobe, Hyogo 650-0047, Japan

[2]Department of Mechanical and Aerospace Engineering,
University of Virginia, 122 Engineer's Way, Charlottesville,VA 22904, USA

[3]Chair of Solid-State and Quantum Chemistry, RWTH Aachen University, 52056 Aachen, Germany

[4]Computational Condensed Matter Physics Laboratory,
RIKEN, Wako, Saitama 351-0198, Japan

[5]Computational Quantum Matter Research Team,
RIKEN Center for Emergent Matter Science (CEMS), Wako, Saitama 351-0198, Japan

*Corresponding author. E-mail: khazaei@riken.jp

The results of phonon spectra for 82 different MAX phases

Cr_2AlC

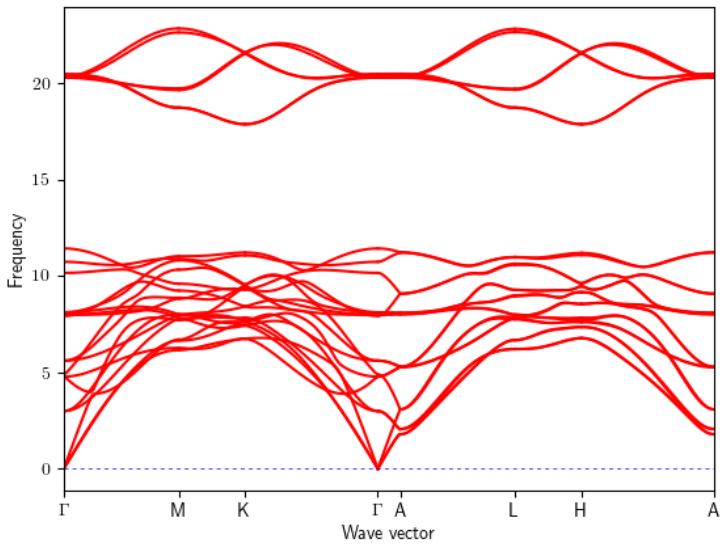

Cr_2GaN

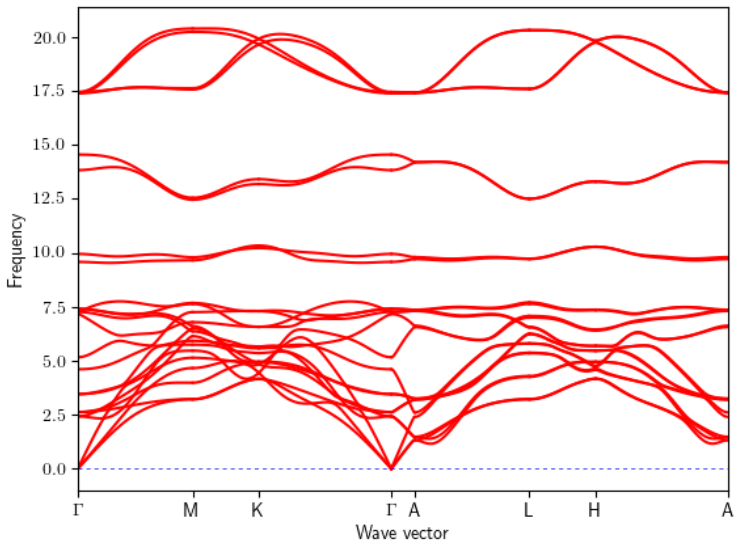

Cr_2GaC

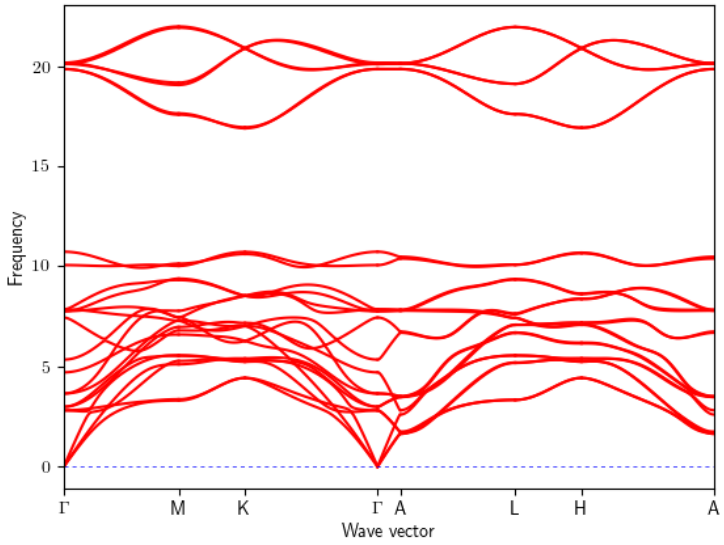

Cr_2GeC

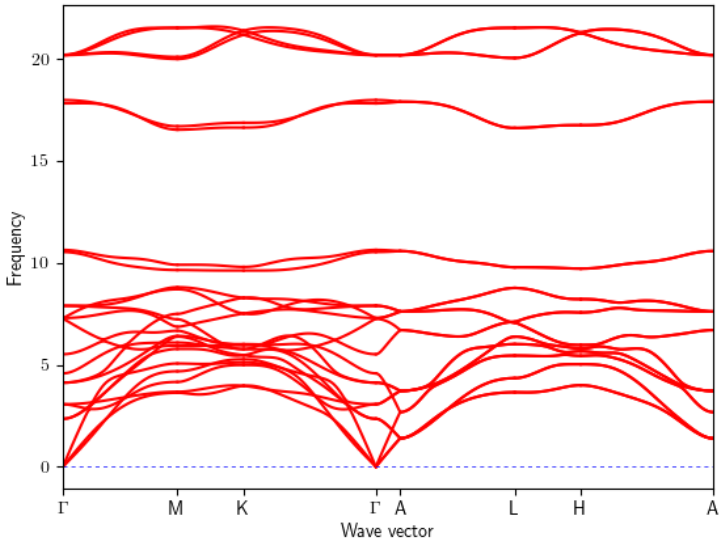

Cr_2TiAlC_2

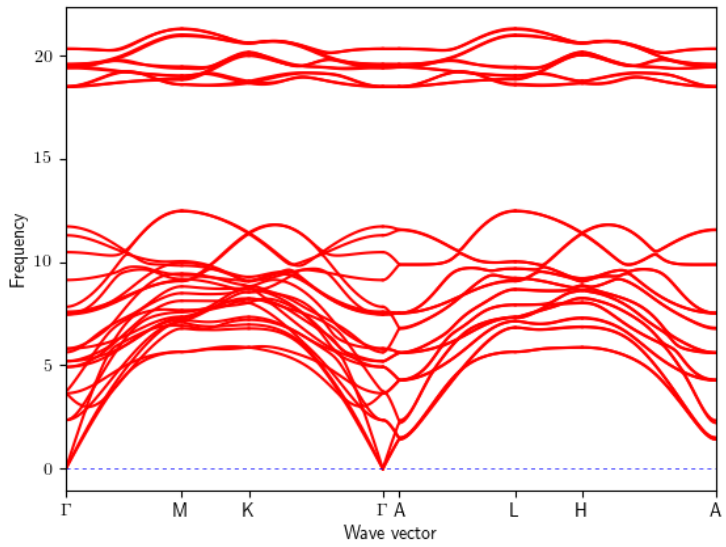

Hf_2AlC

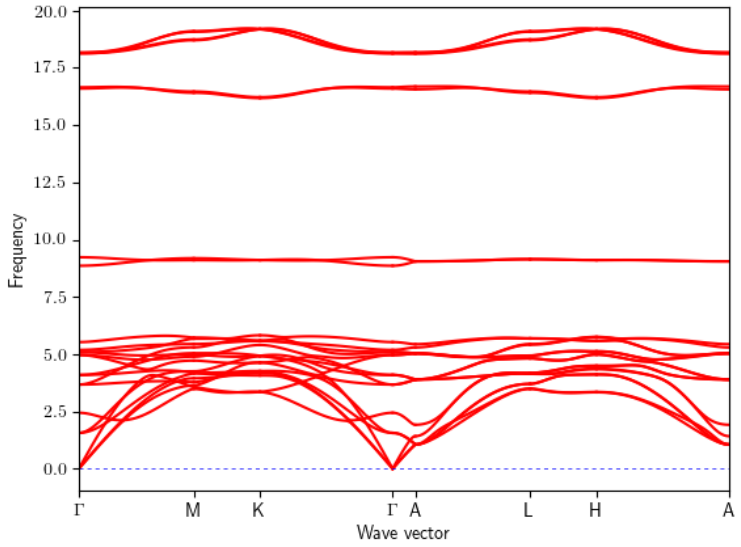

Hf_2AlN

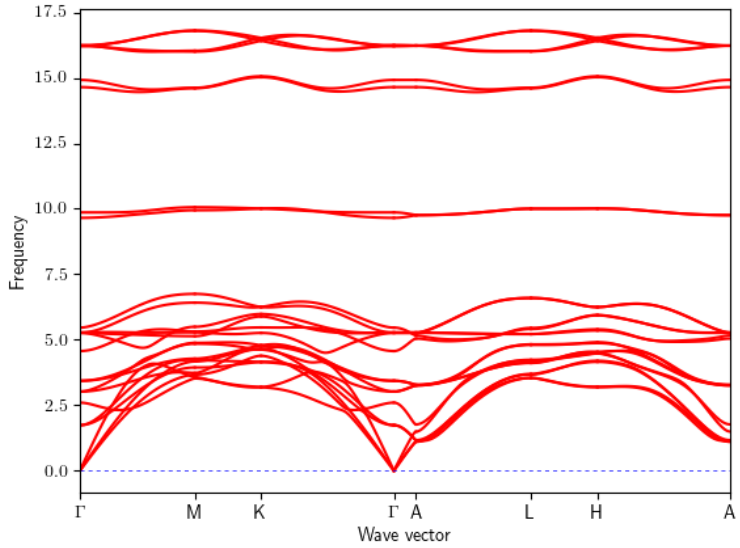

Hf_2InC

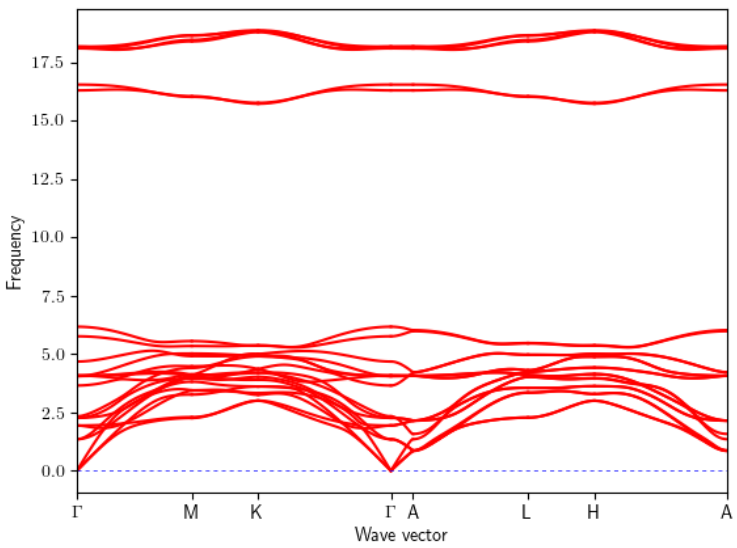

Hf_2PbC

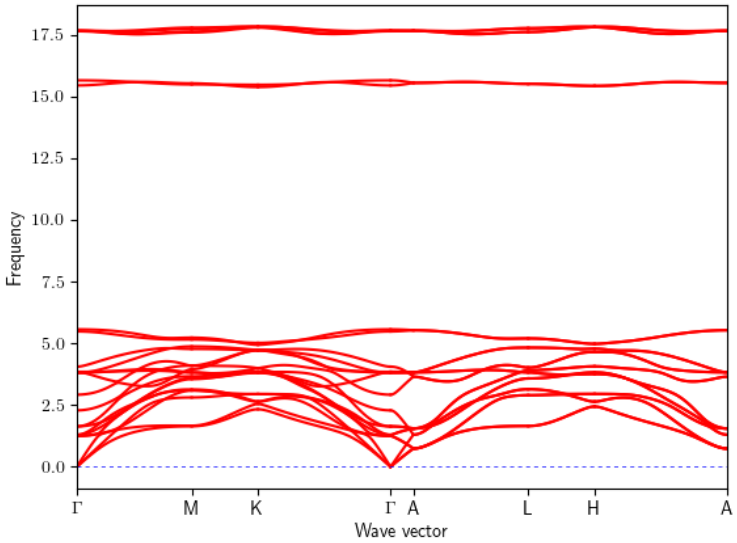

Hf_2SnC

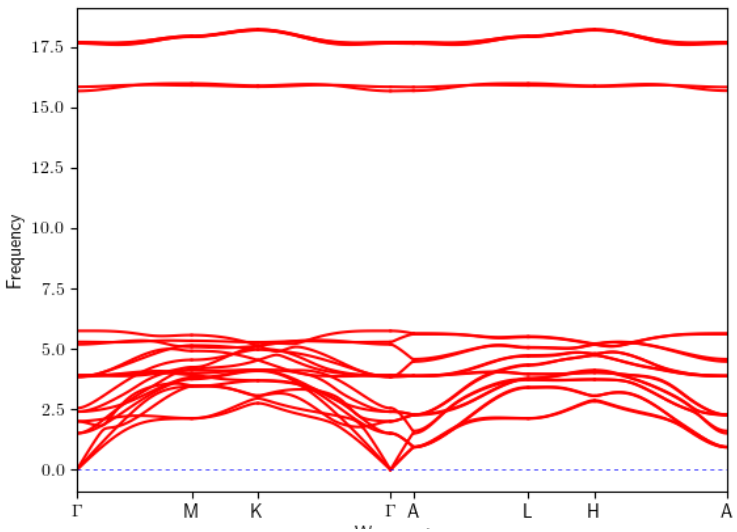

Hf_2SC

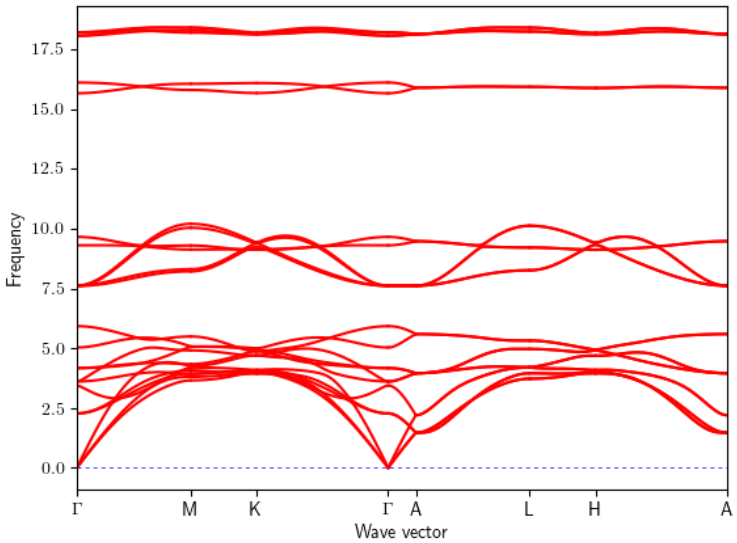

Hf_2SnN

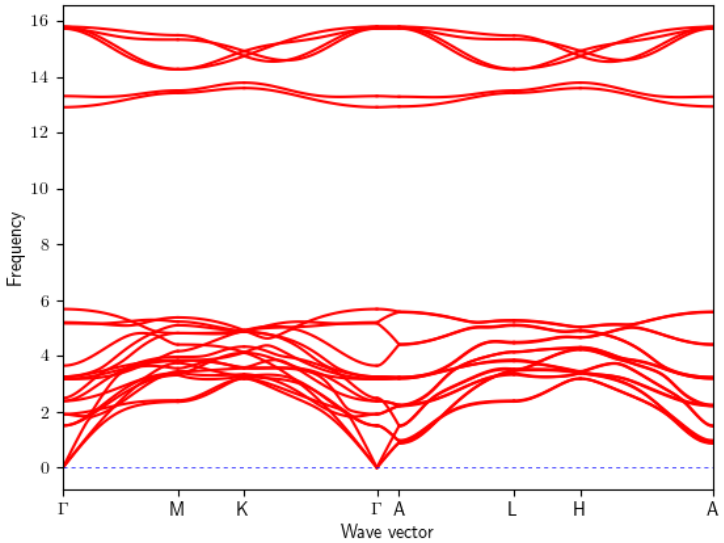

Hf_2TlC

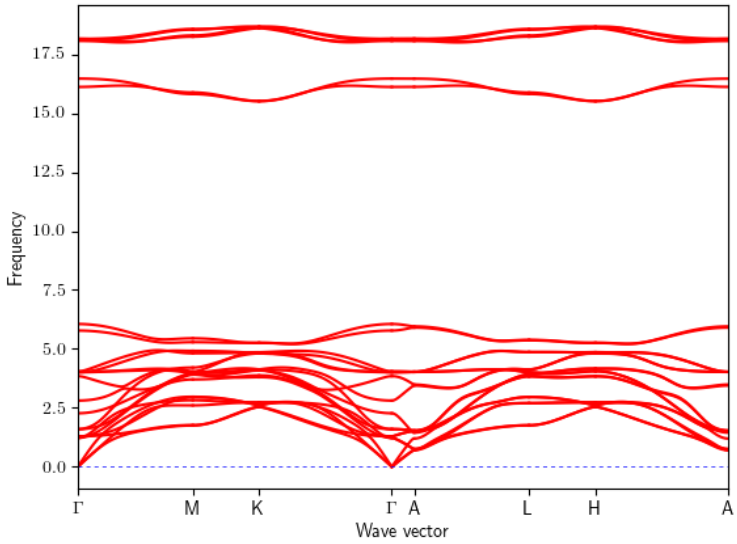

Mo_2ScAlC

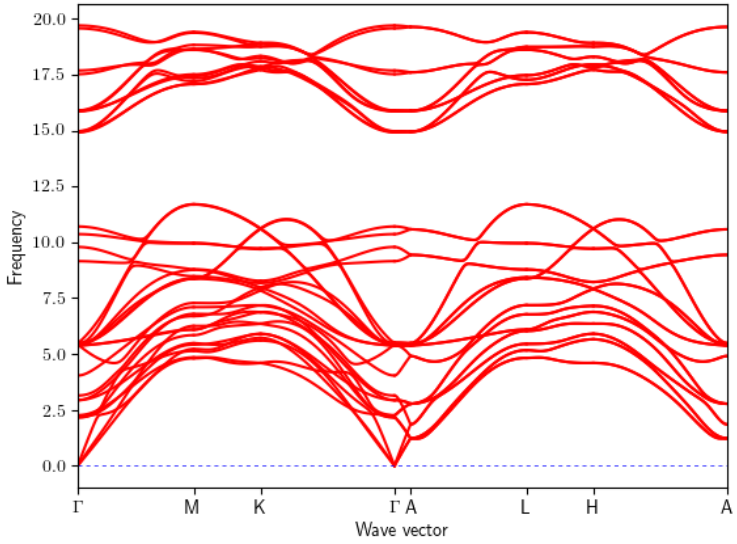

Mo_2GaC

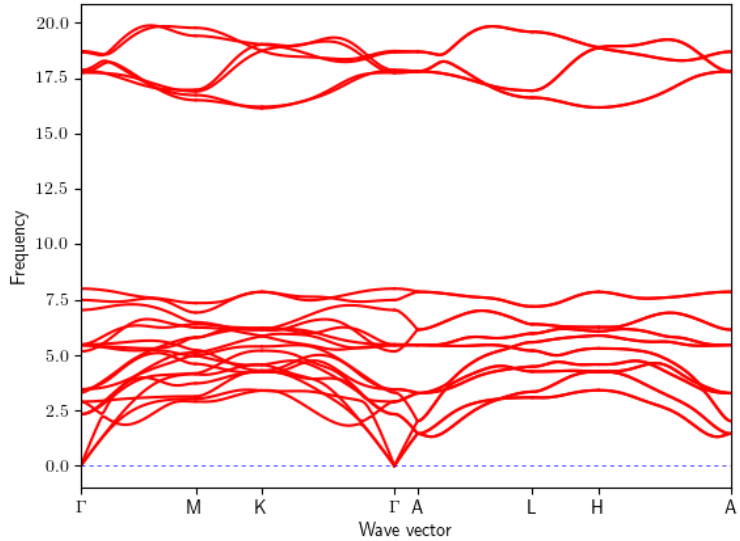

Mo_2TiAlC

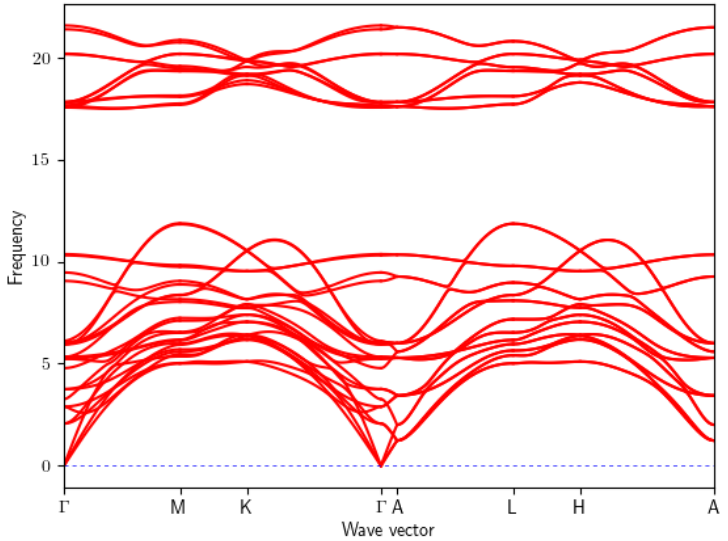

Mo_2Ti_2AlC

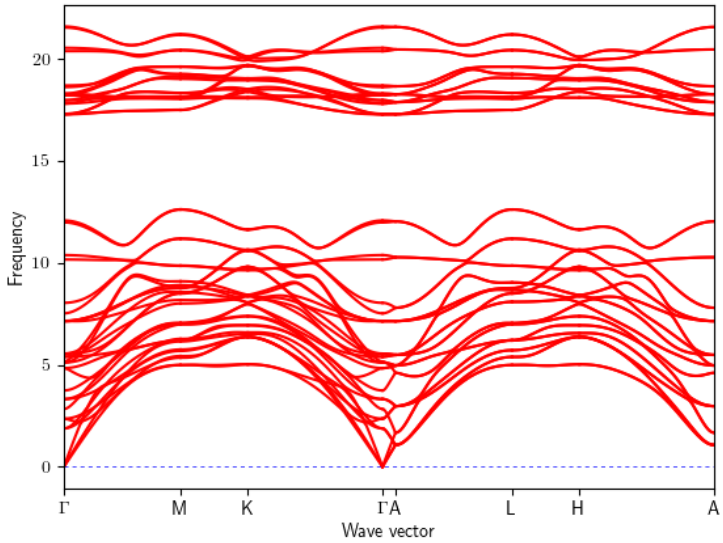

Nb_2GaC

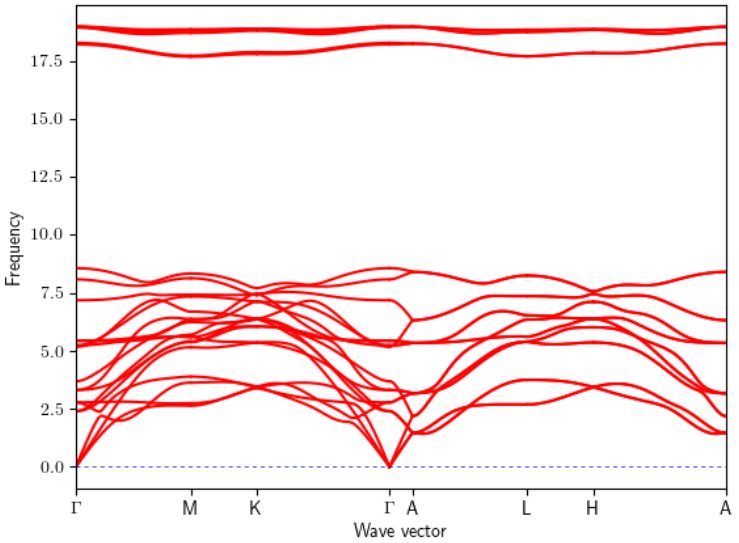

Nb_2AlC

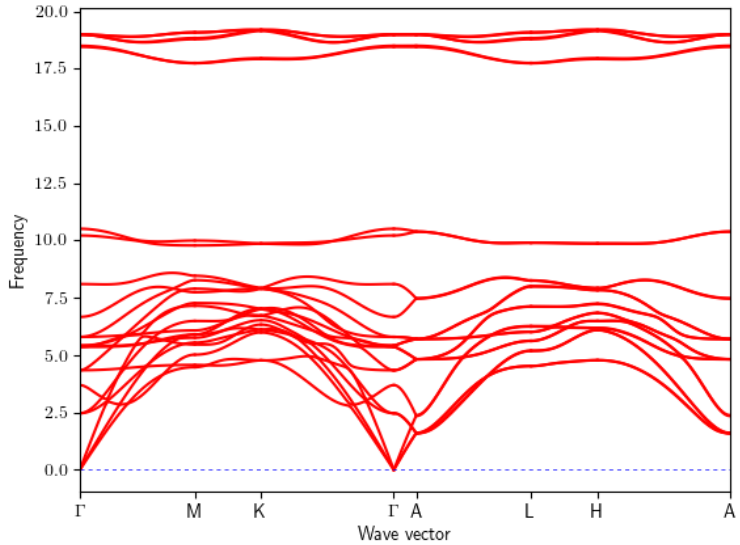

Nb_2InC

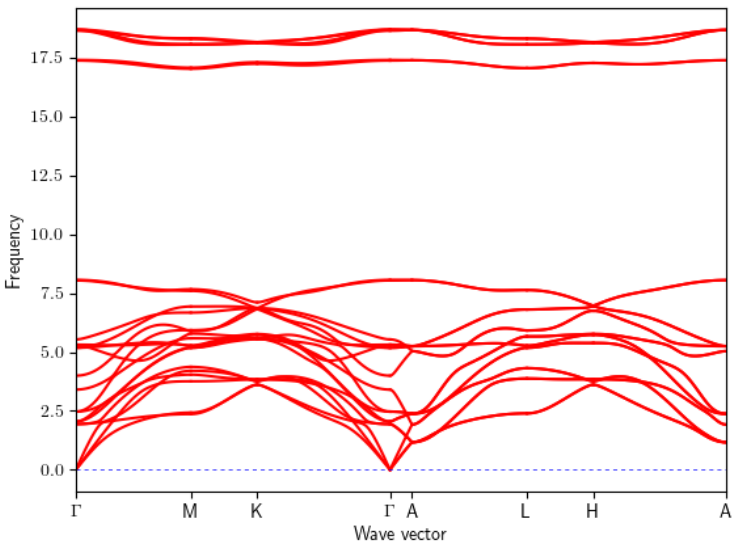

Nb_2PC

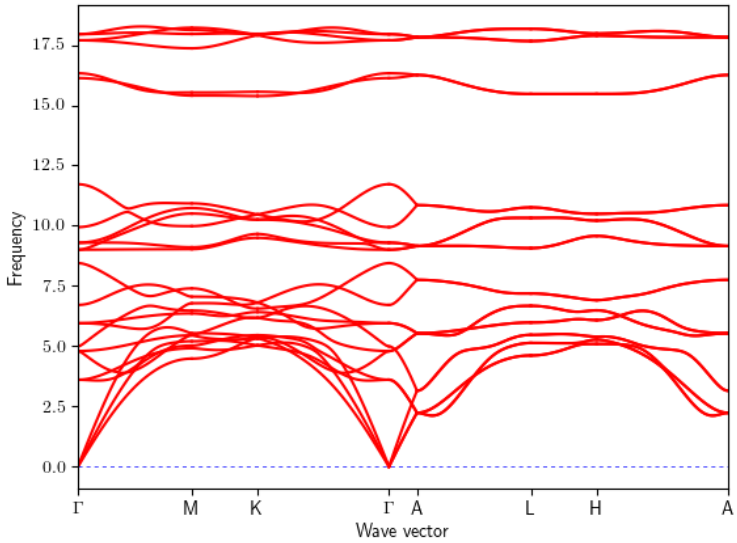

Nb_2SnC

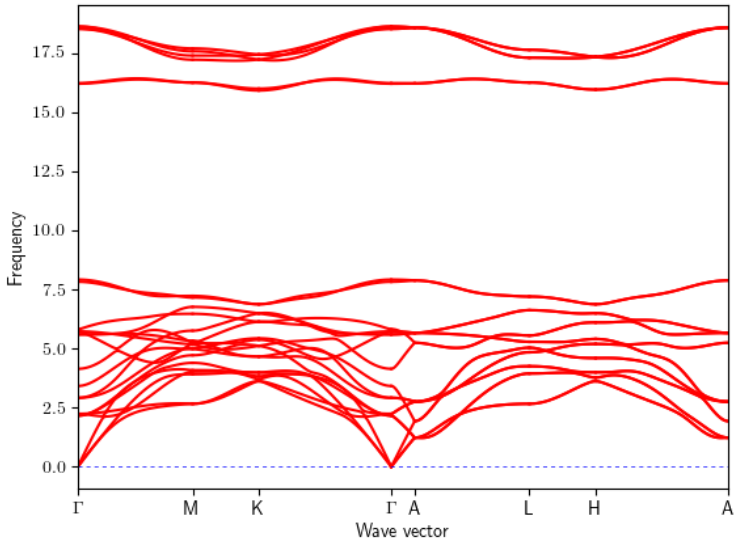

Nb_2SC

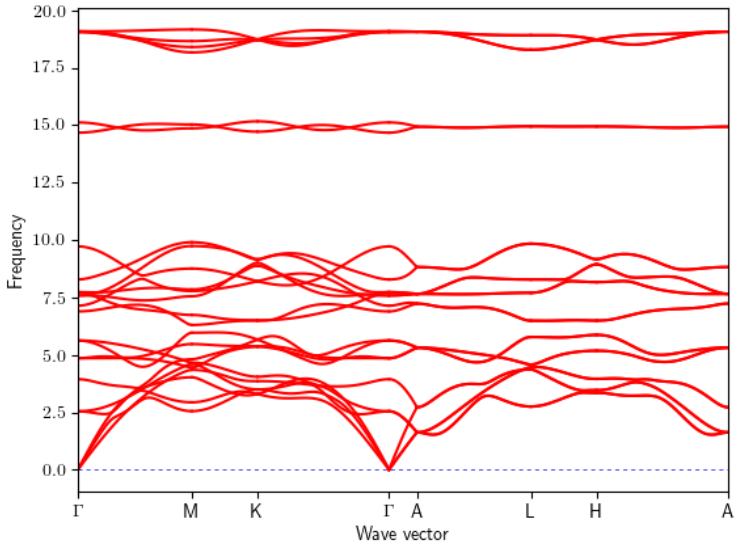

Nb_3SiC_2

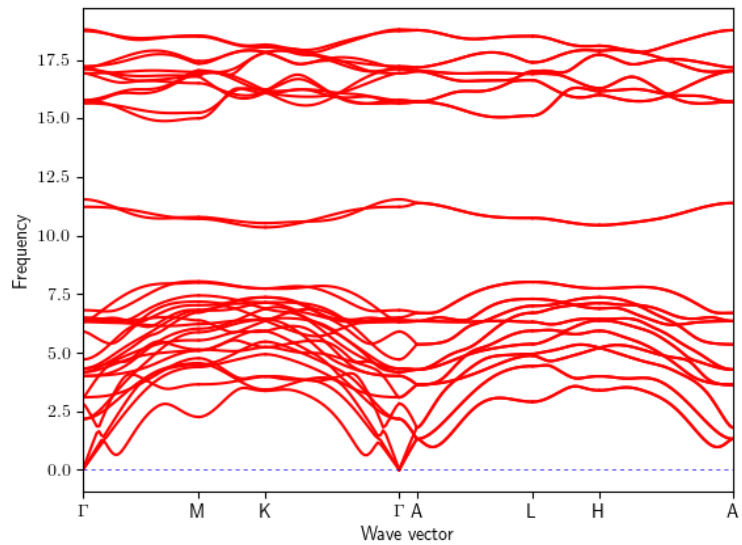

Nb_4AlC_3

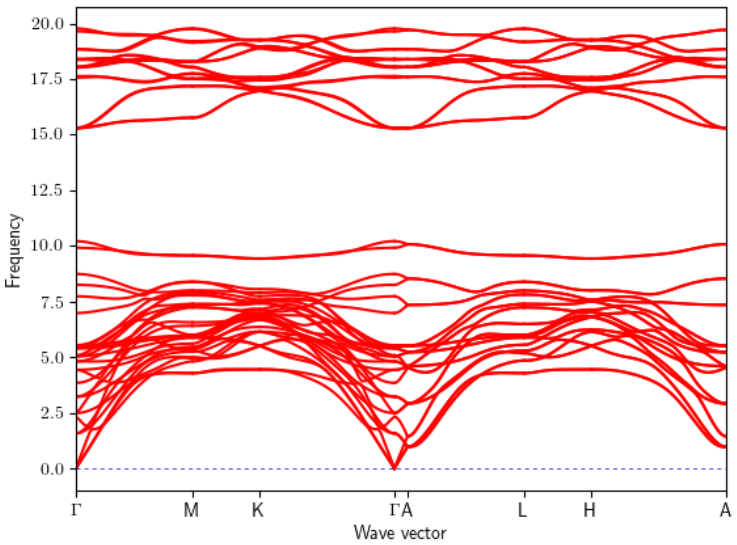

Sc_2AlC

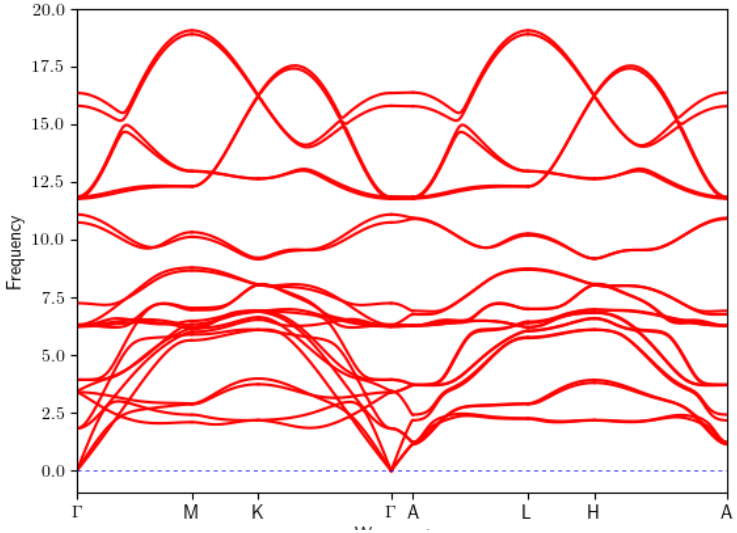

Nb_5AlC_4

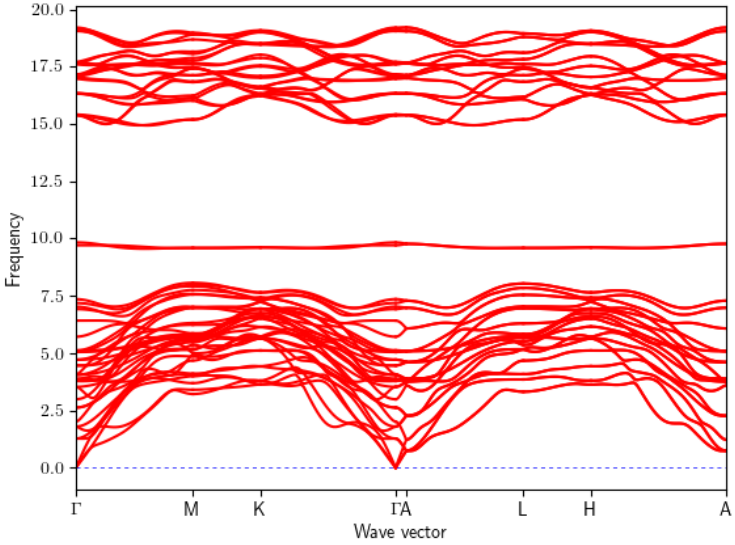

Sc_2GaC

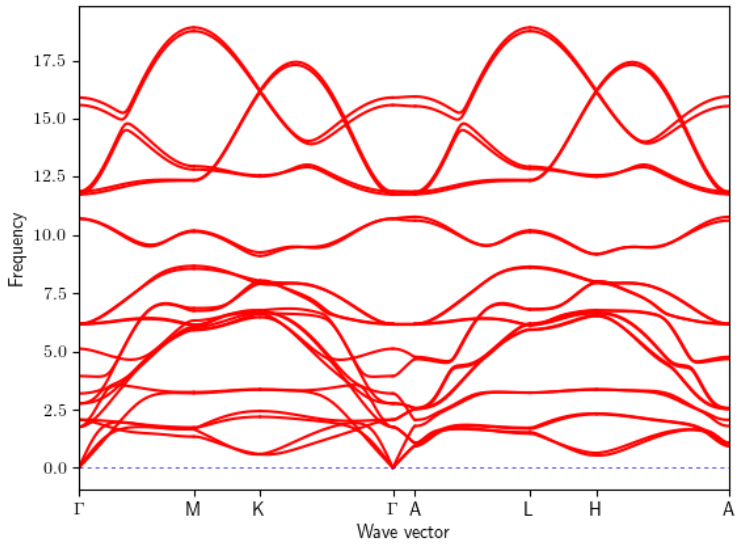

Sc_2InC

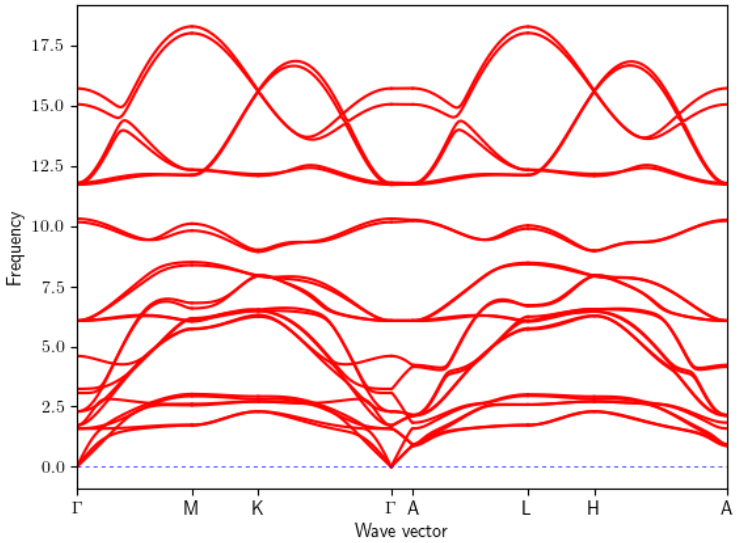

Ta_2AlC

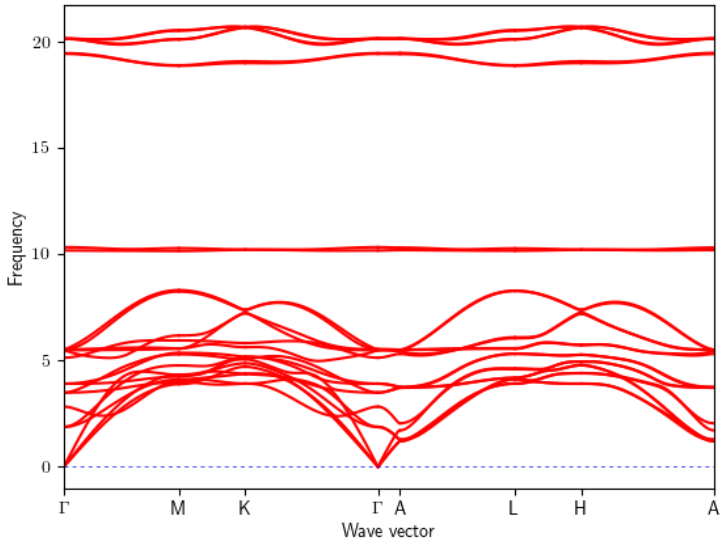

Sc_2TlC

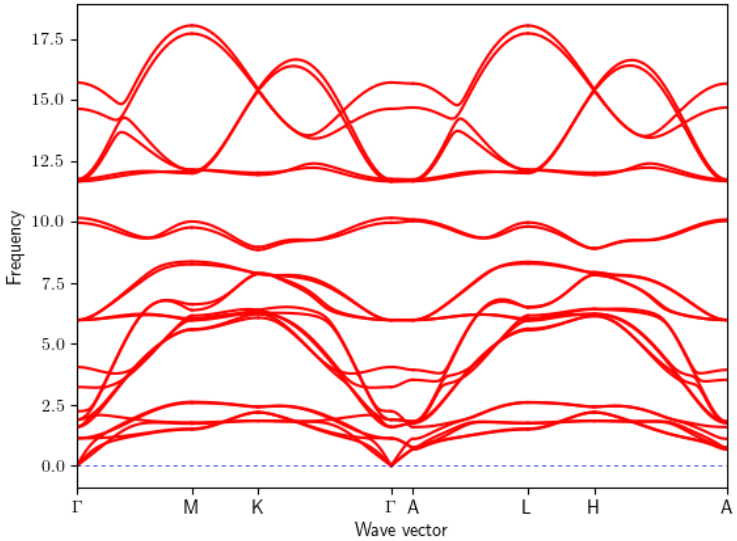

Ta_2GaC

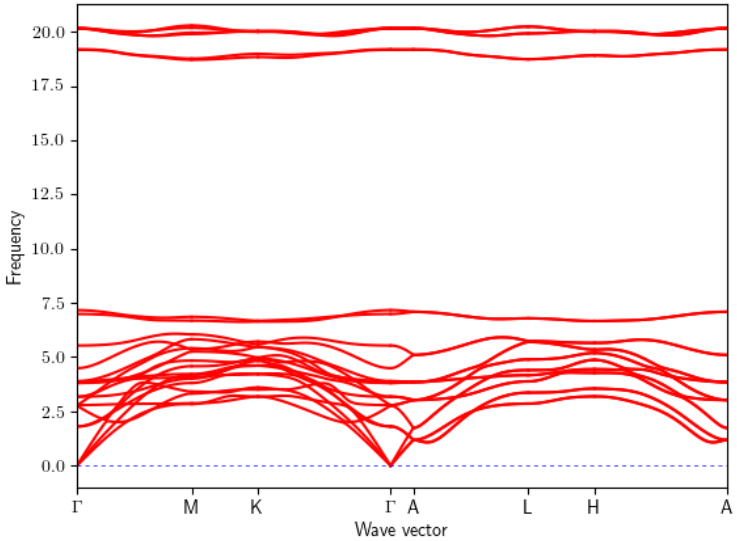

Ta_3AlC_2

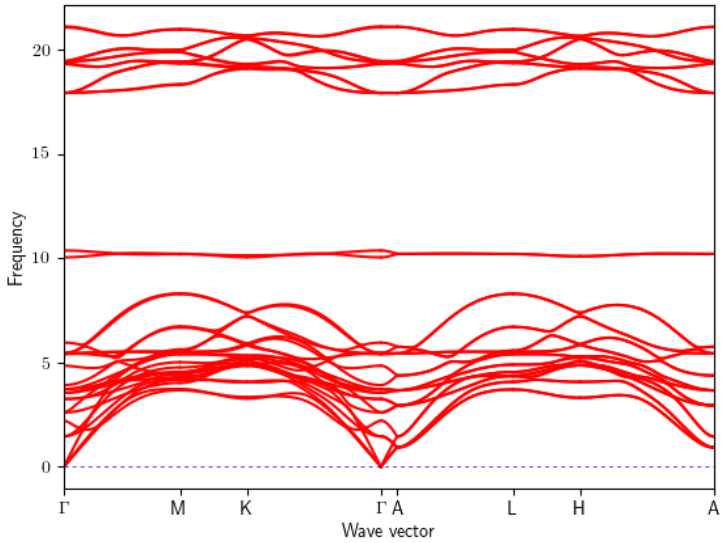

Ta_5AlC_4

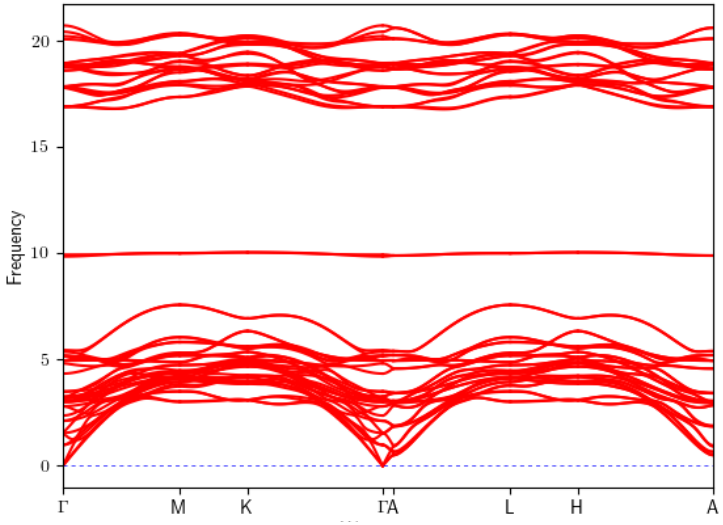

Ta_4AlC_3

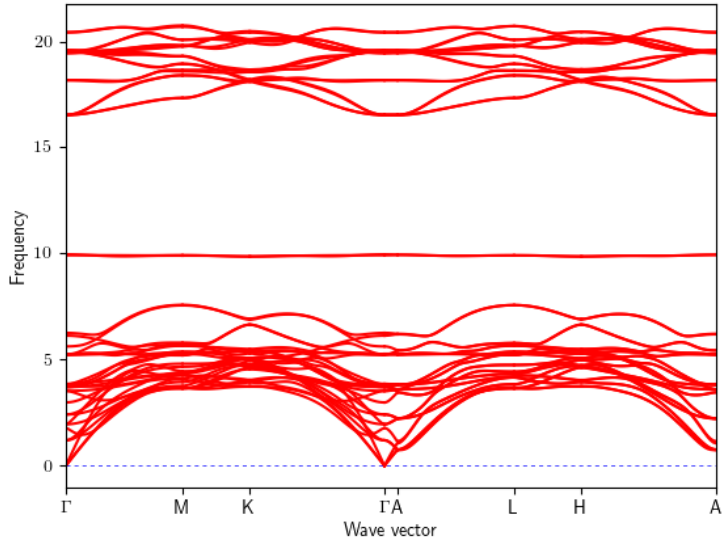

Ti_2AlC

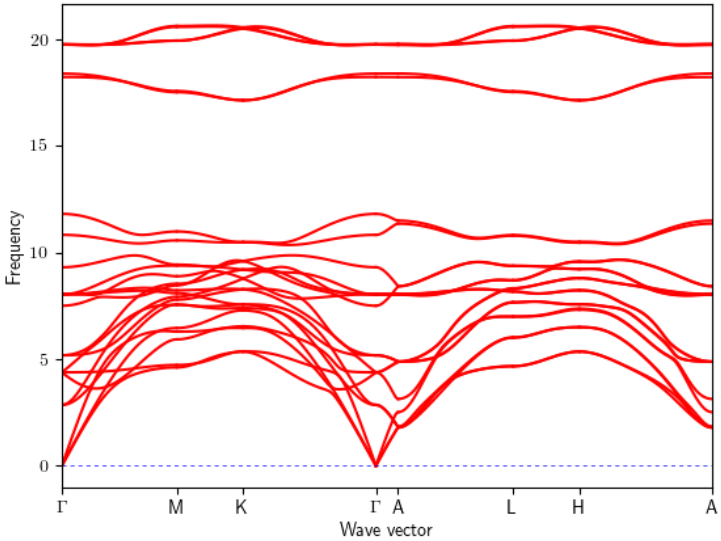

Ti_2AlN

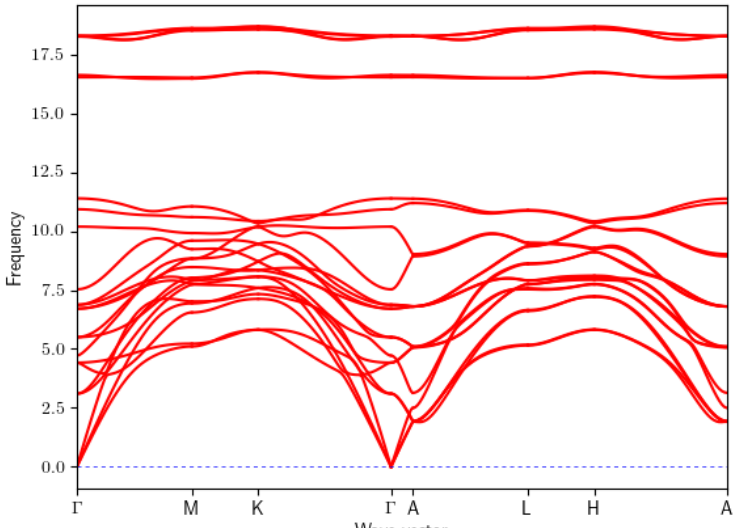

Ti_2CdC

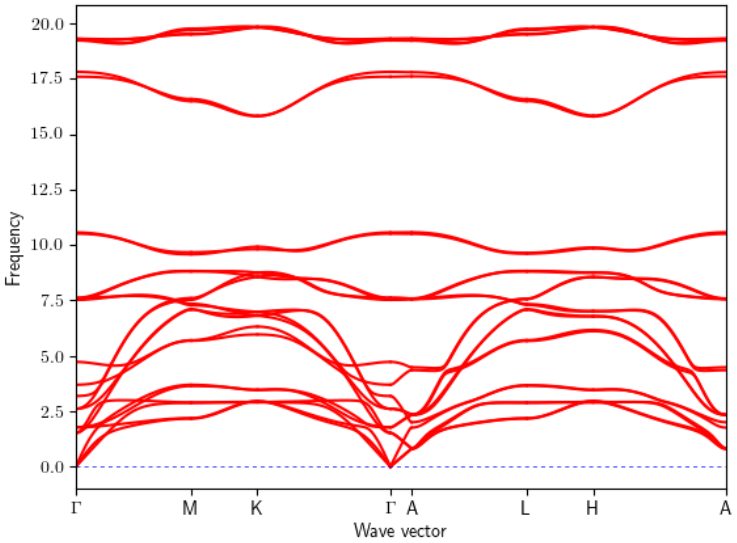

Ti_2AsC

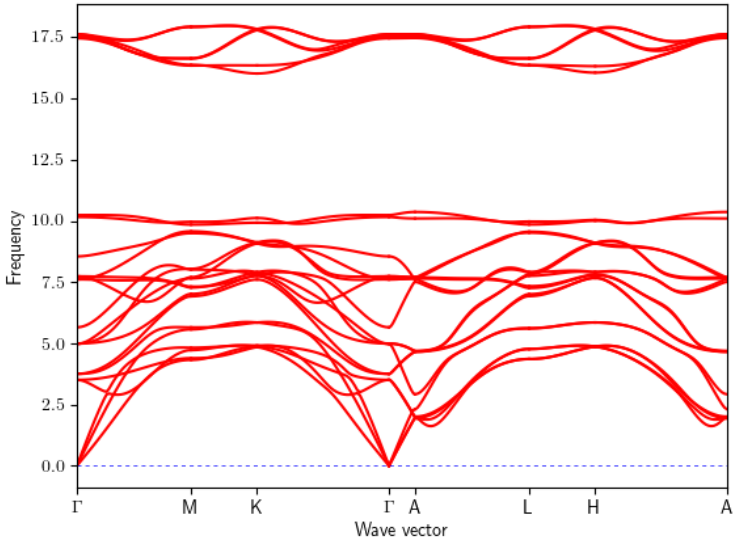

Ti_2GaC

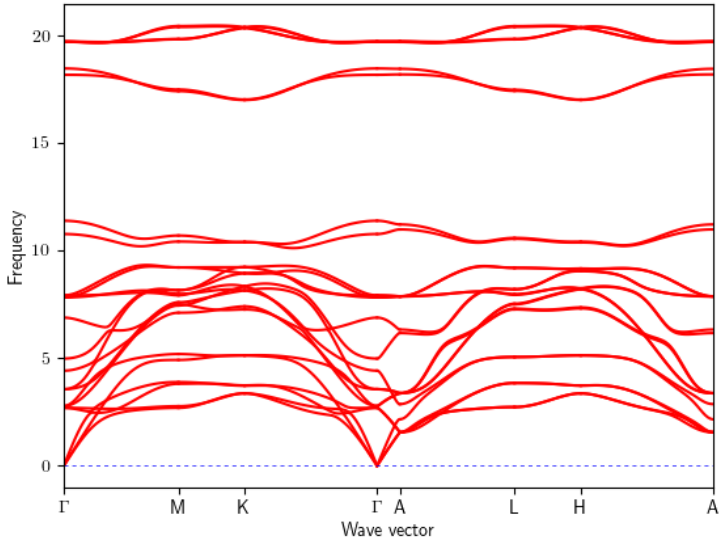

Ti_2GaN

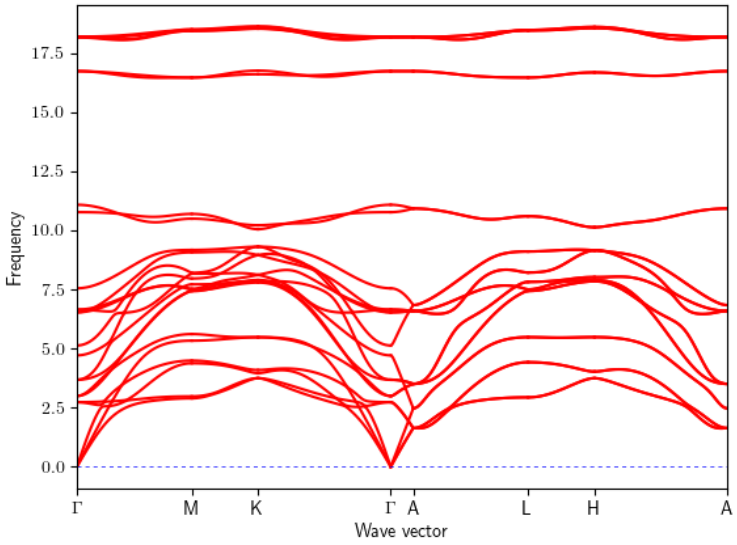

Ti_2InC

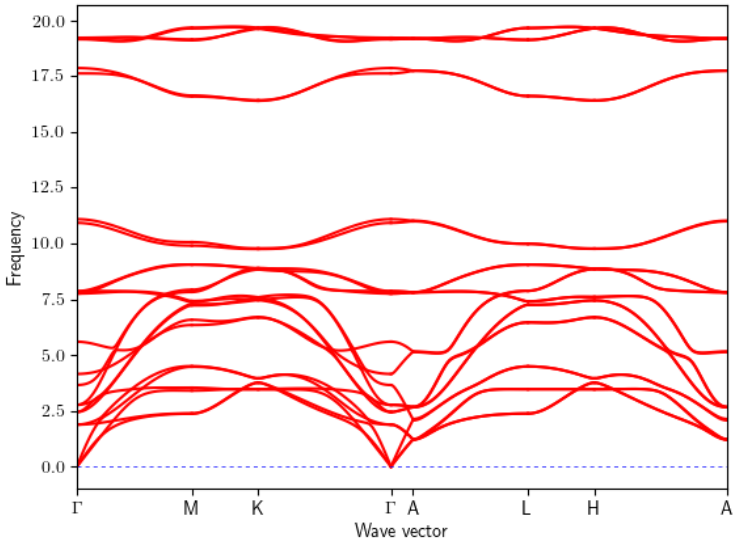

Ti_2GeC

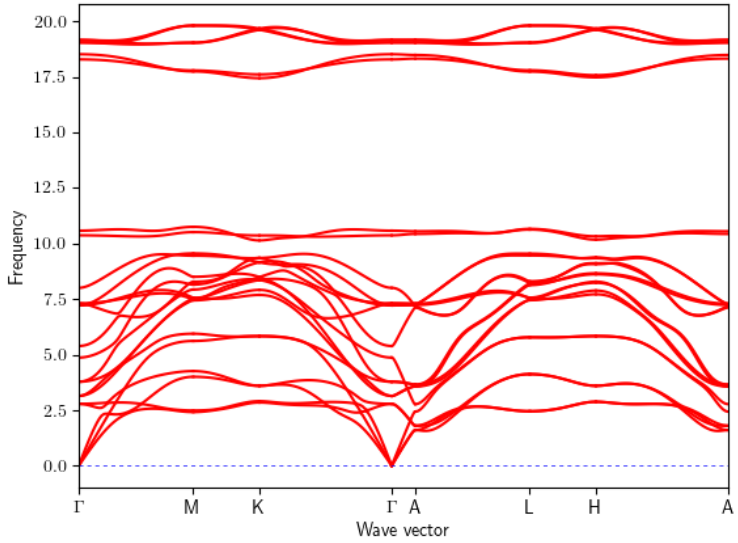

Ti_2InN

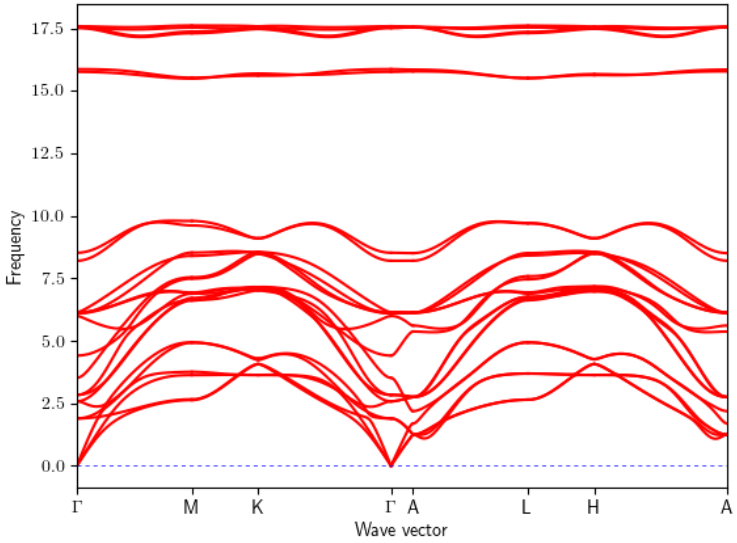

Ti_2PbC

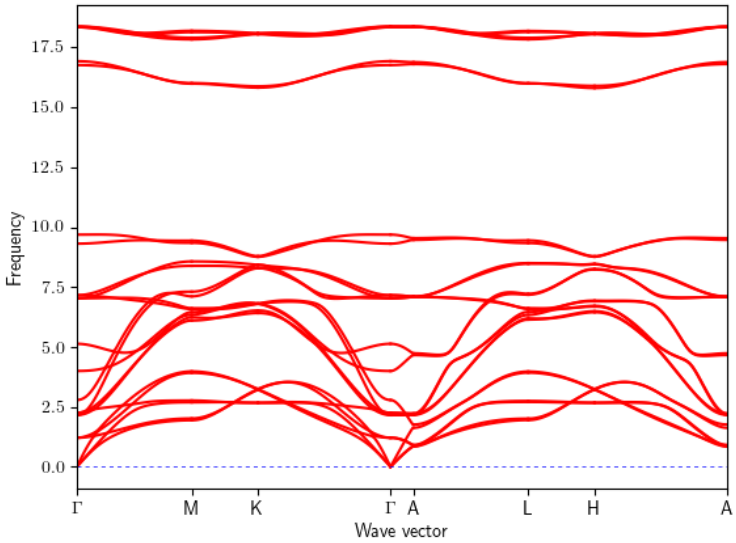

Ti_2SC

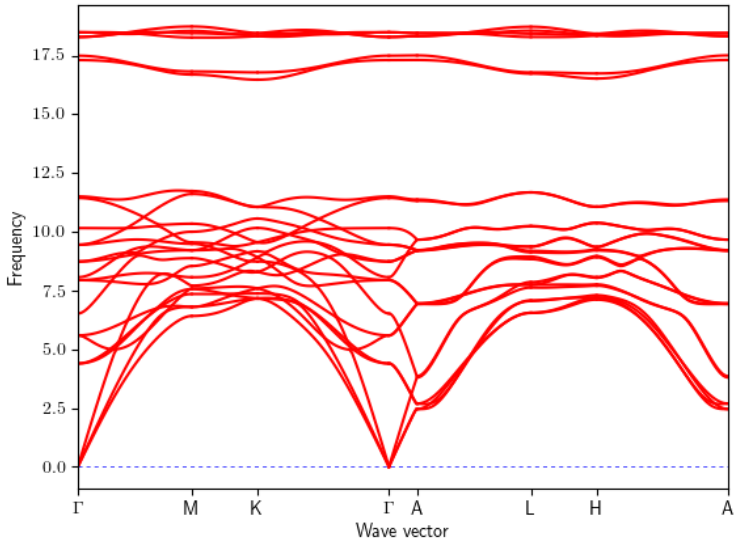

Ti_2PC

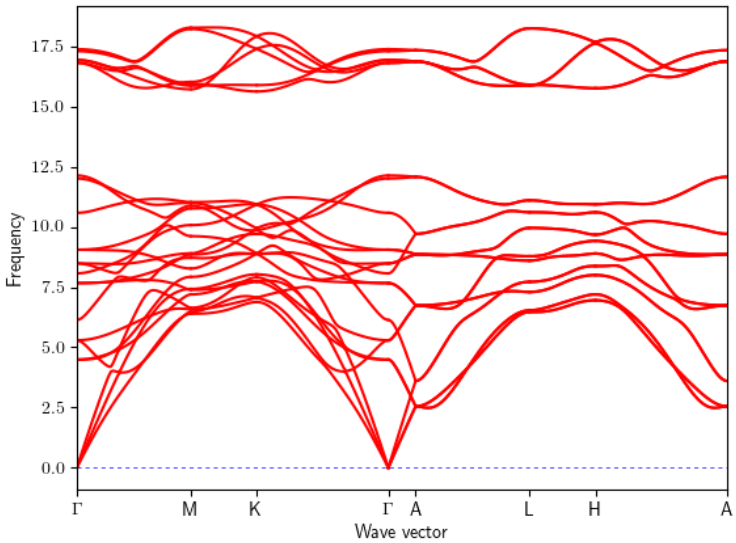

Ti_2SiC

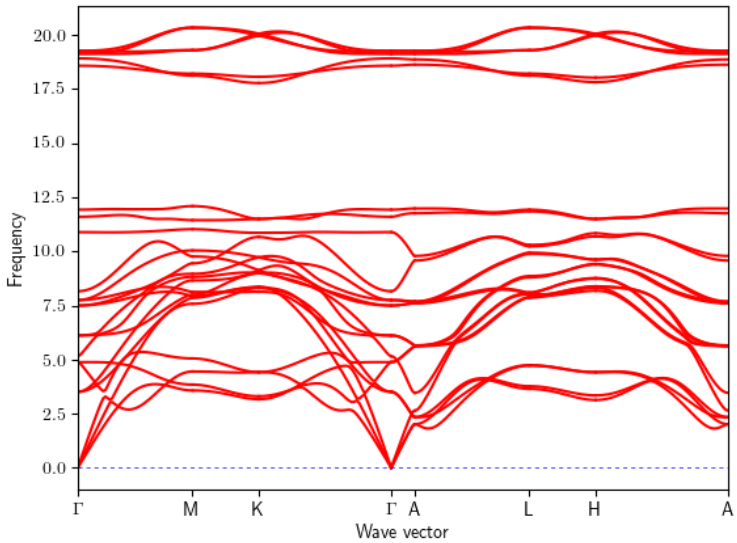

Ti_2SnC

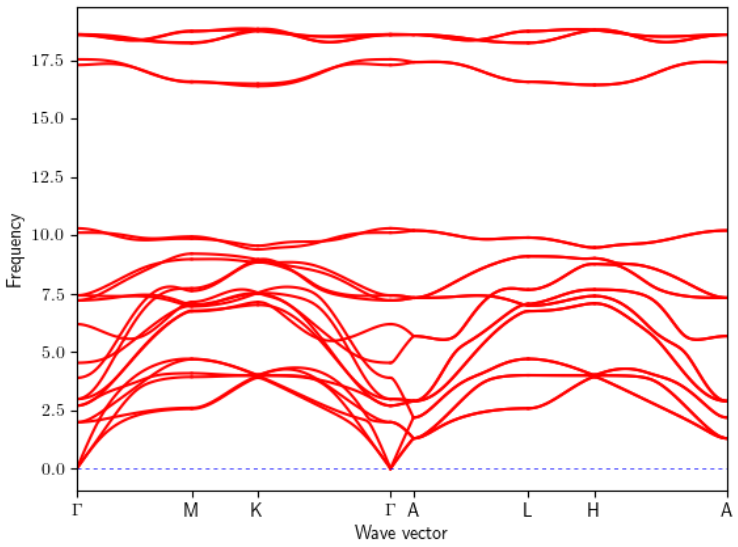

Ti_3AlC_2

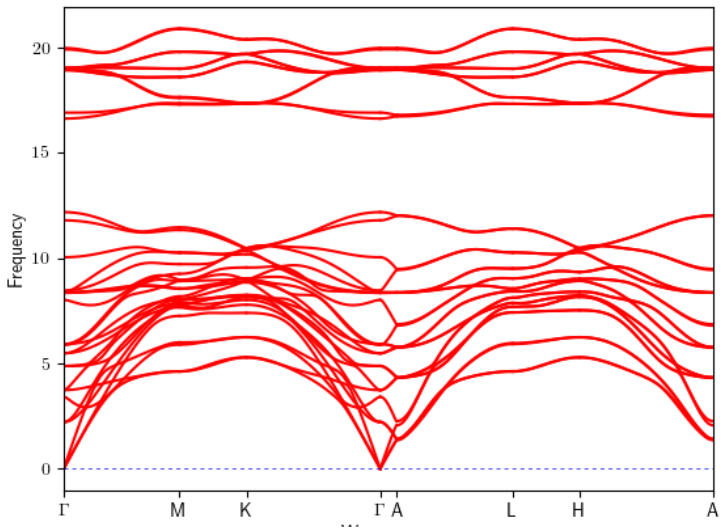

Ti_2TlC

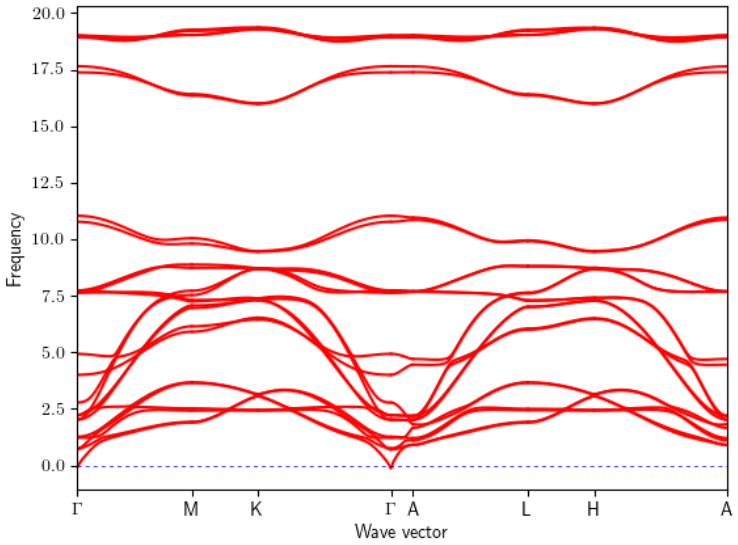

Ti_3AuC_2

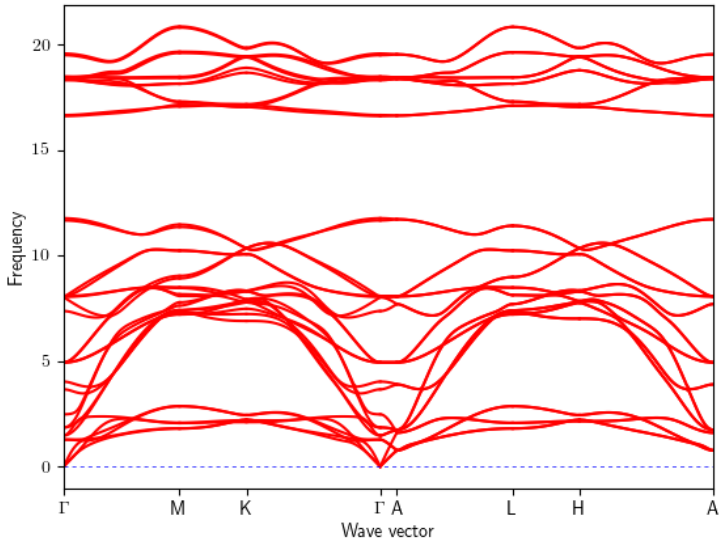

Ti_3GeC_2

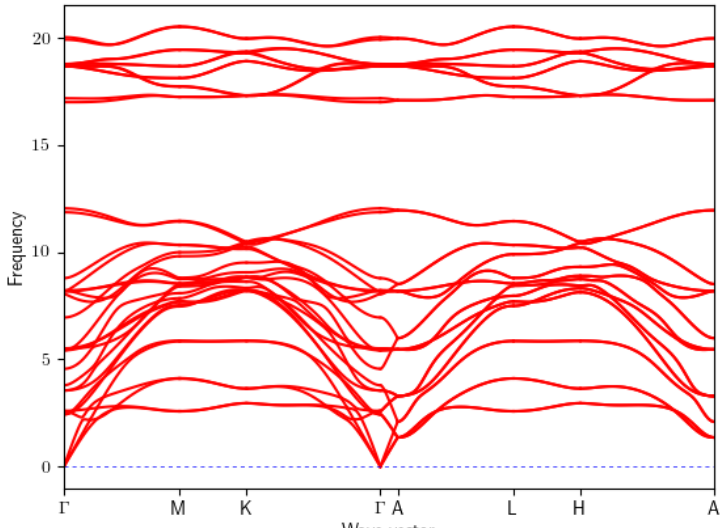

Ti_3SiC_2

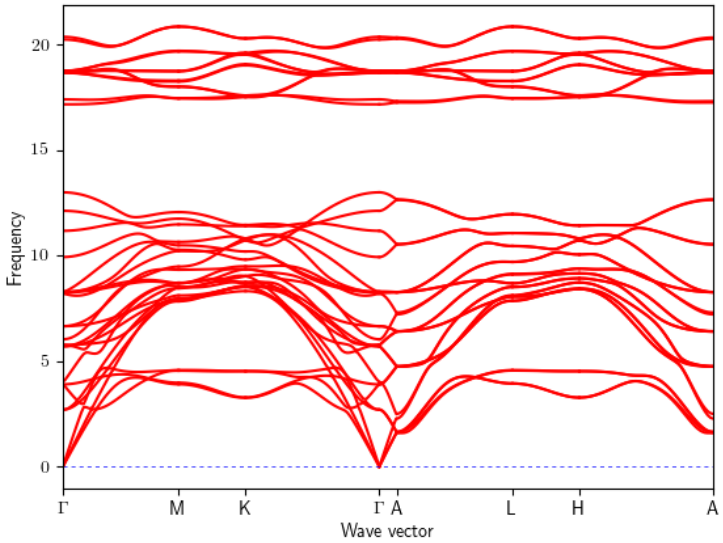

Ti_3IrC_2

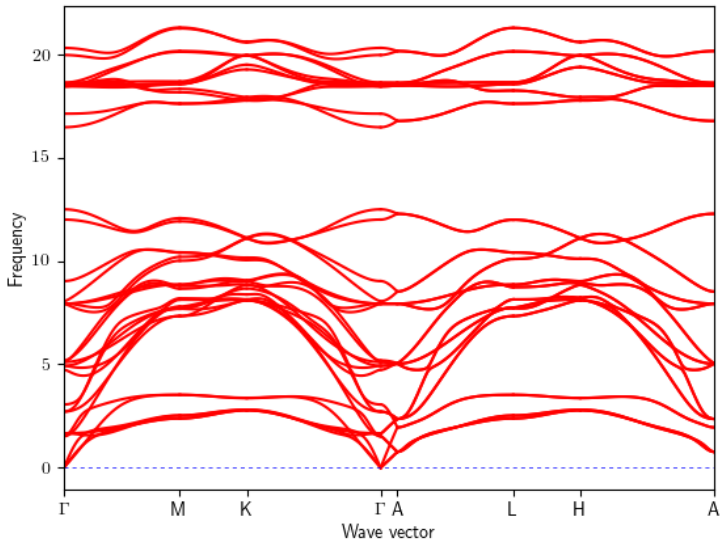

Ti_3SnC_2

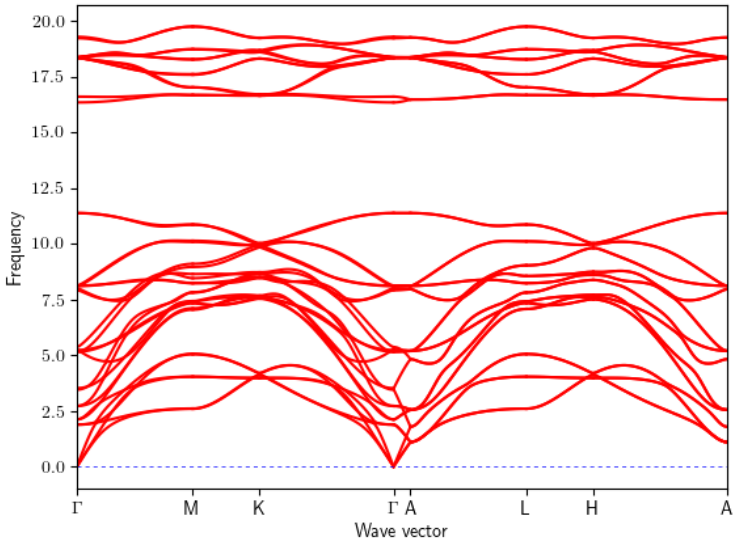

Ti_4AlN_3

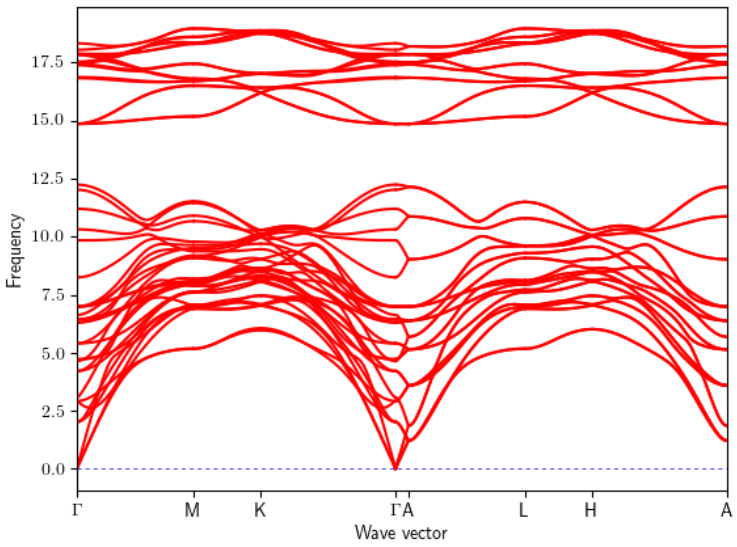

Ti_4GeC_3

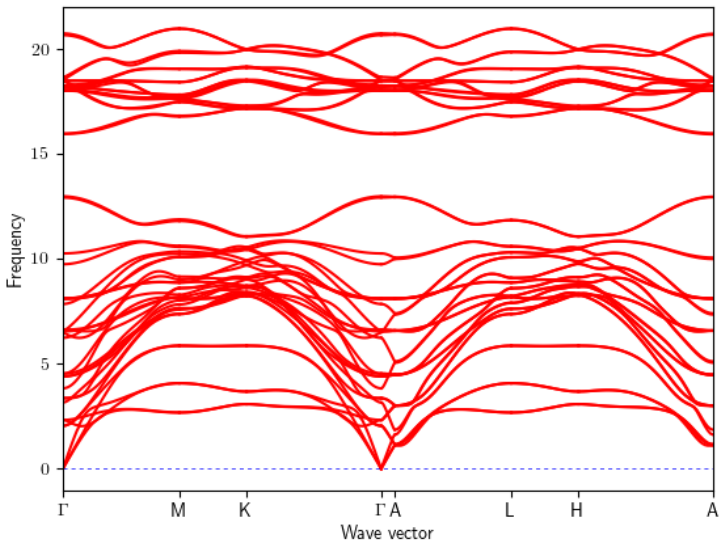

Ti_4GaC_3

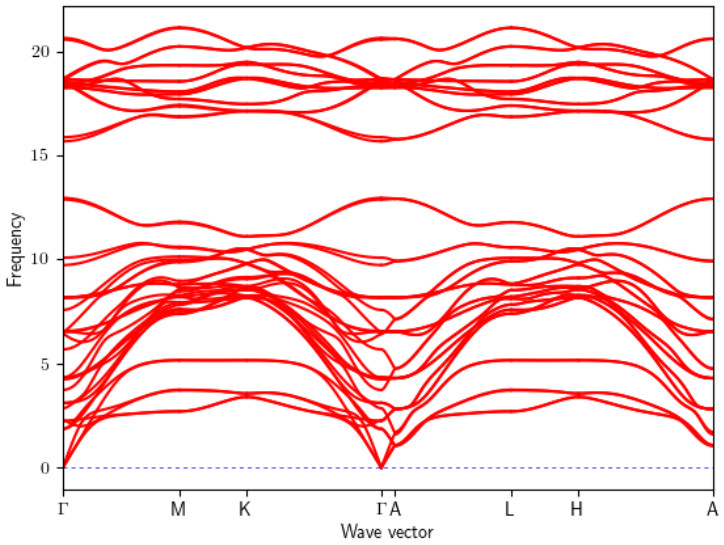

Ti_4SiC_3

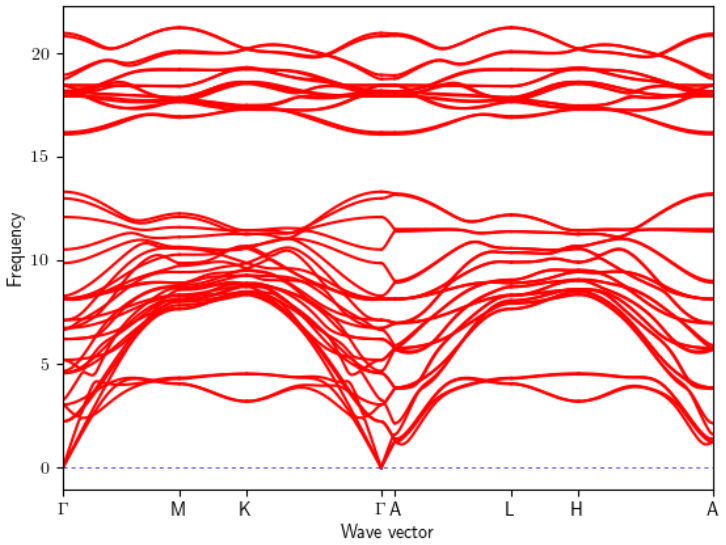

Ti_5AlC_4

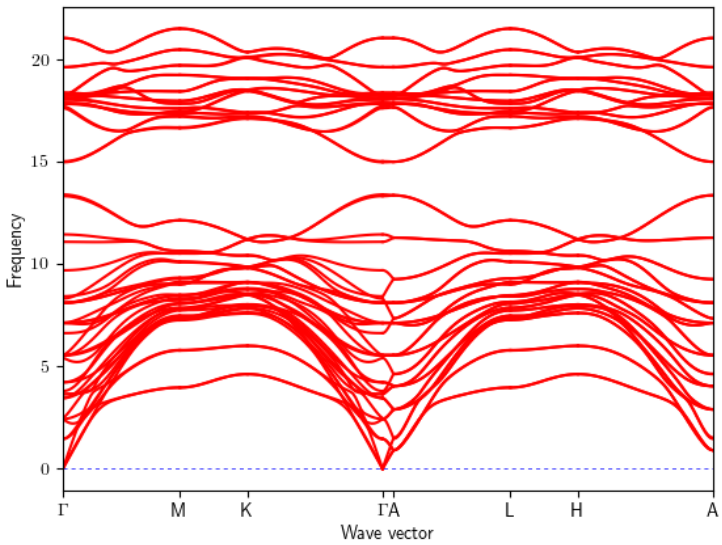

V_2AsC

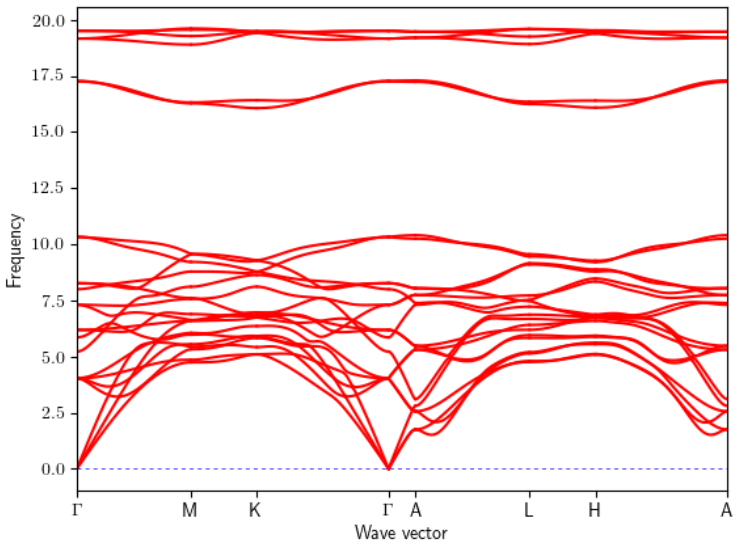

V_2AlC

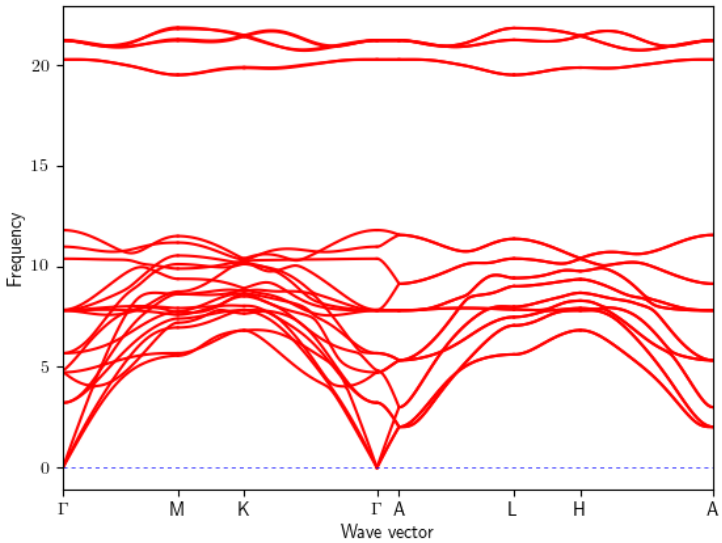

V_2GaC

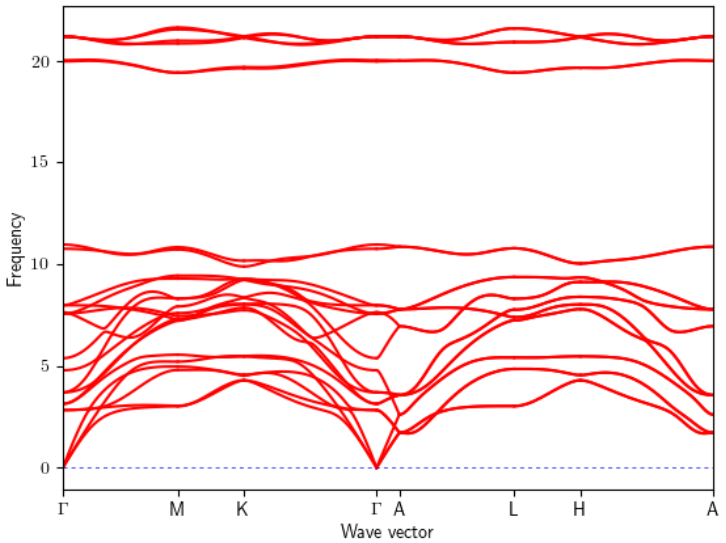

V_2GaN

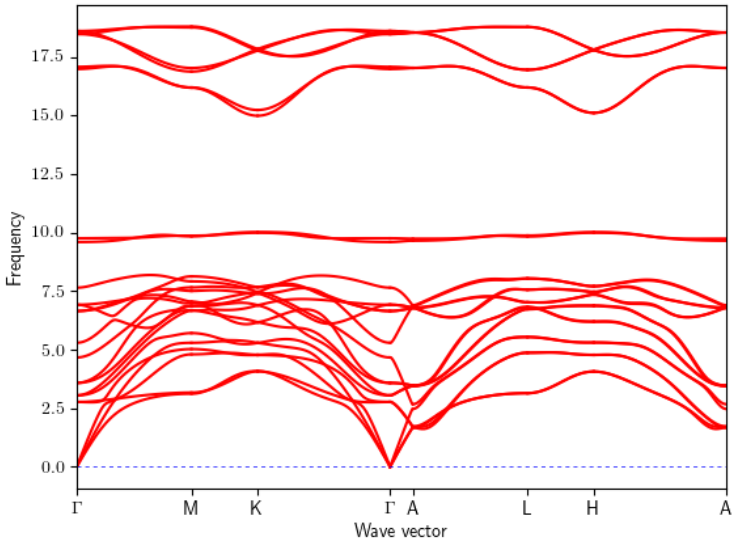

V_2PC

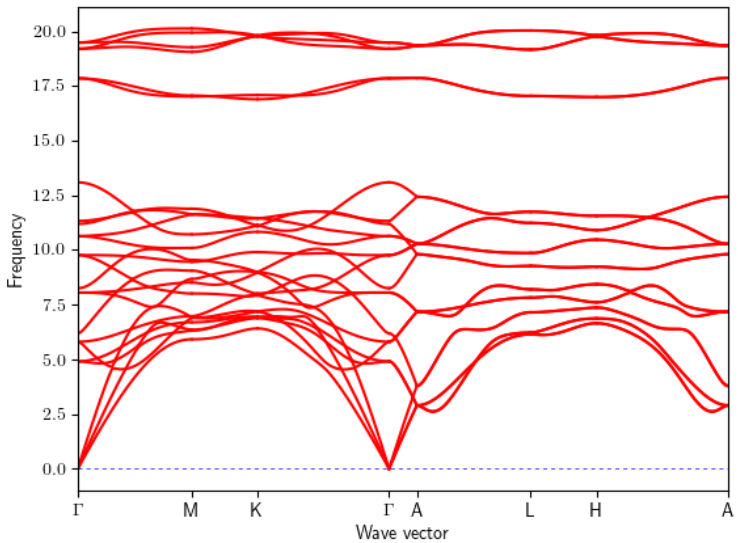

V_2GeC

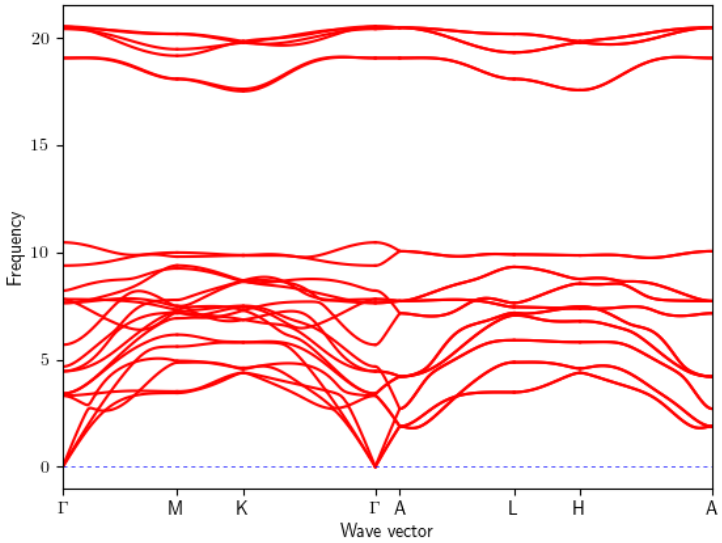

V_2SiC

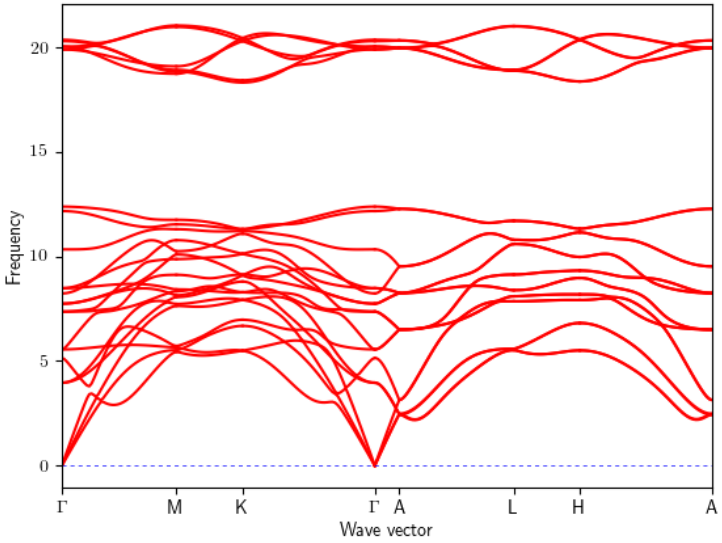

V_3AlC_2

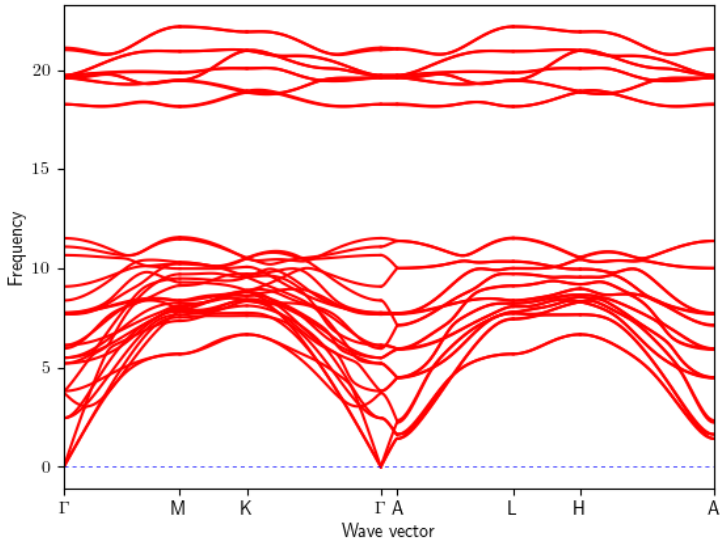

V_4AlC_3

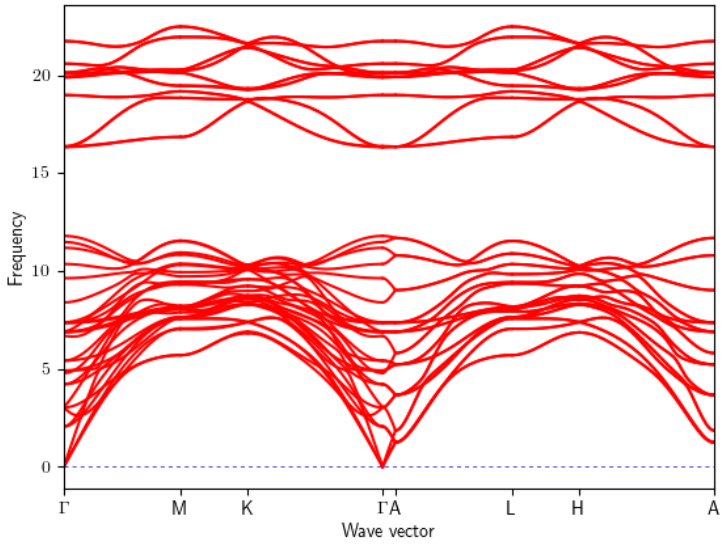

V_3SiC_2

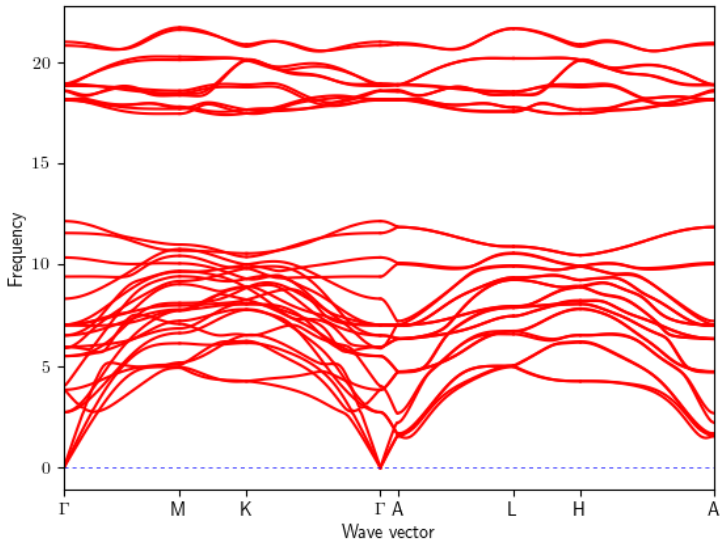

Zr_2AlC

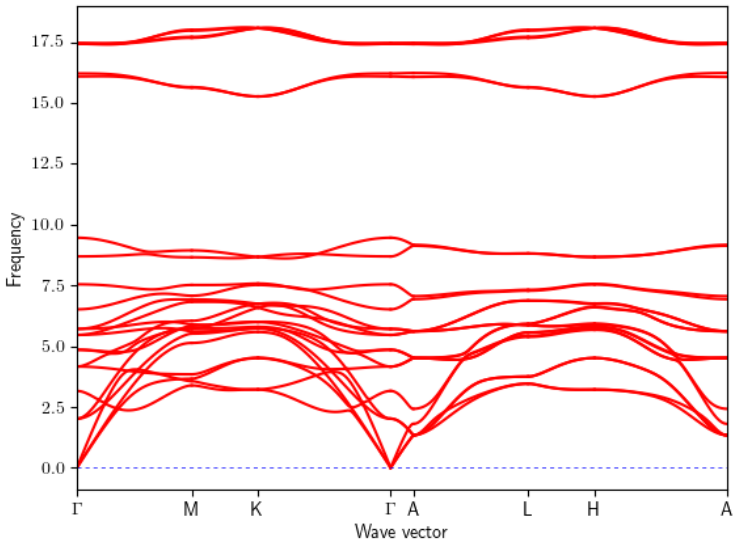

Zr_2AlN

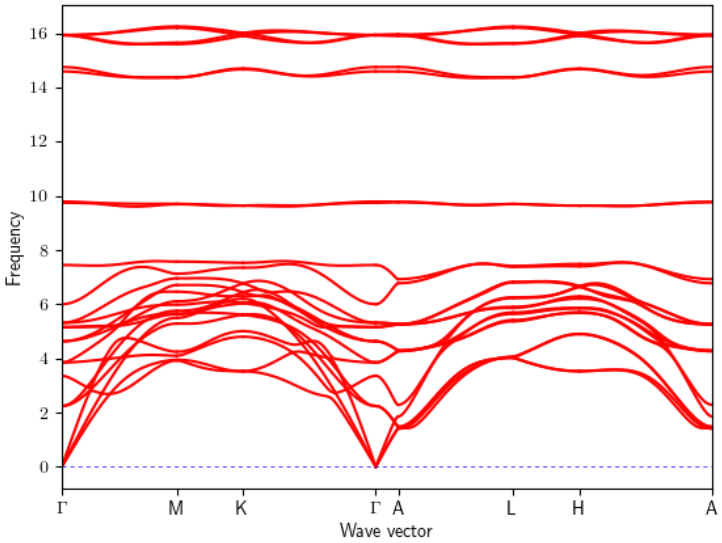

Zr_2InC

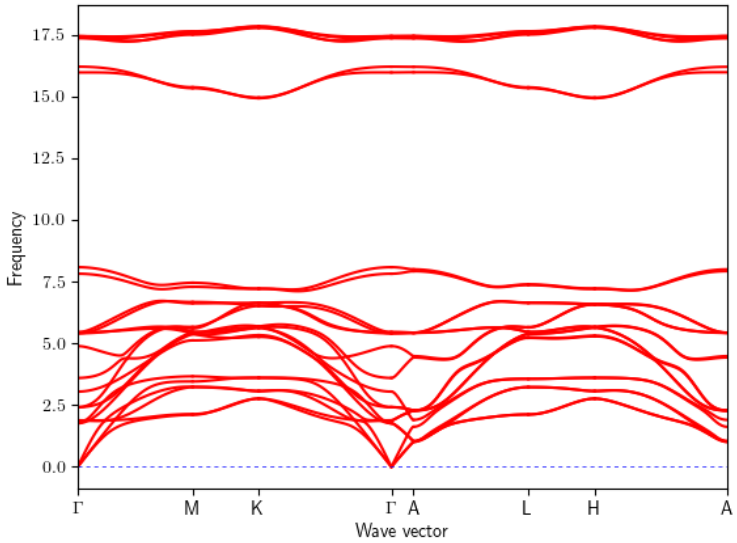

Zr_2BiC

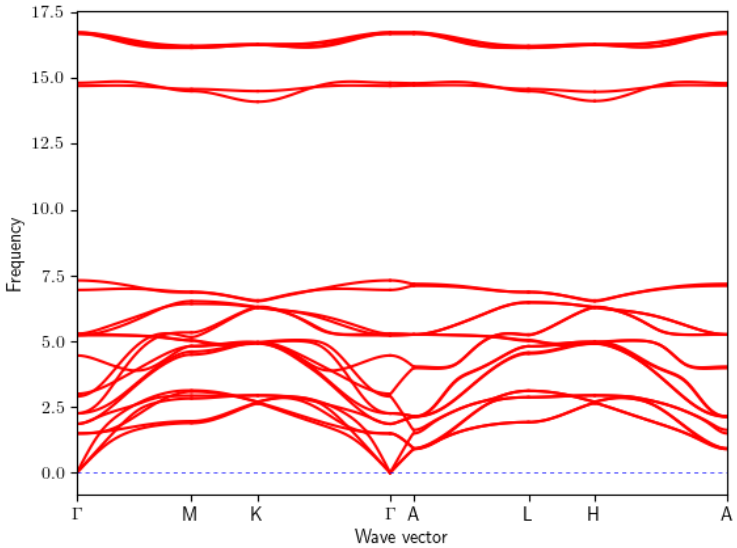

Zr_2InN

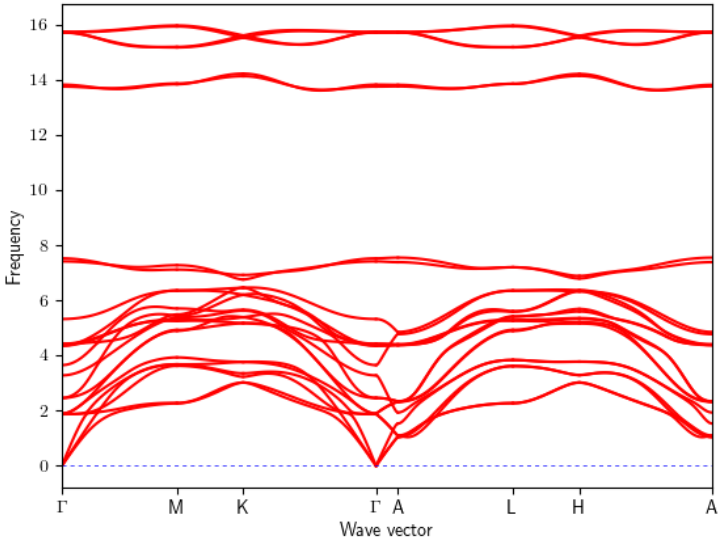

Zr_2PbC

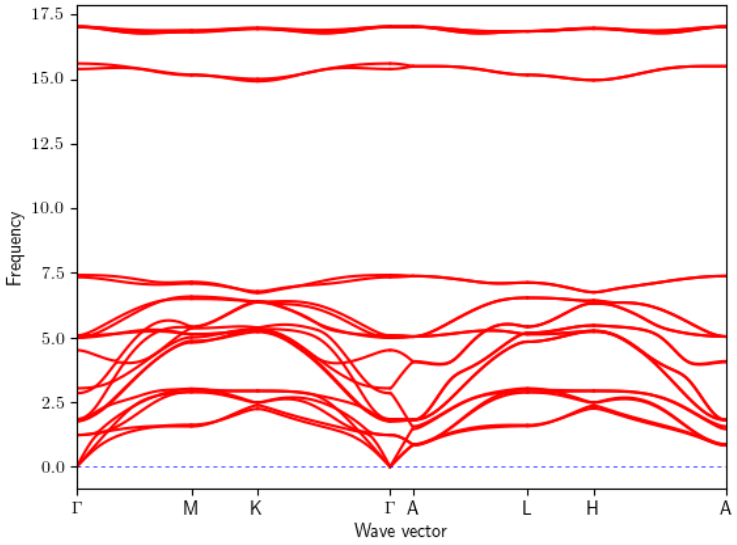

Zr_2SnC

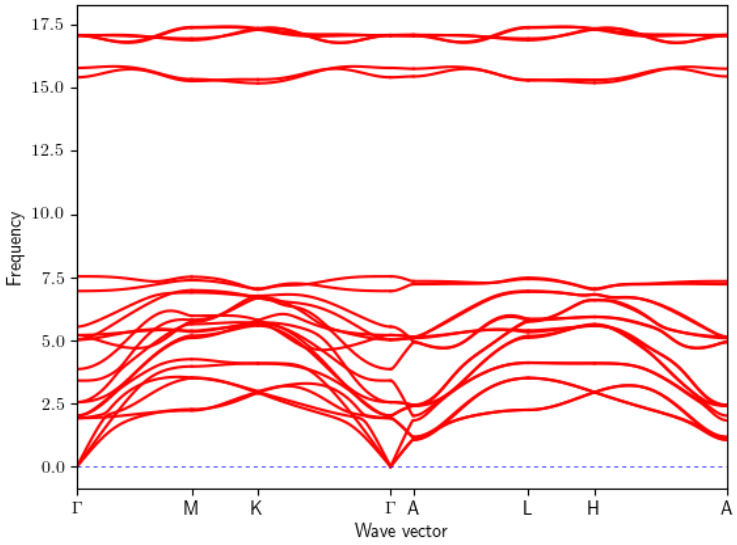

Zr_2SC

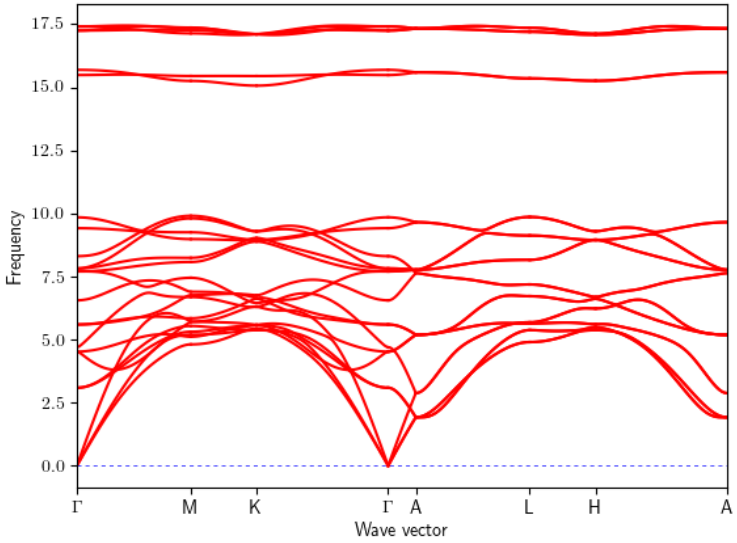

Zr_2TlC

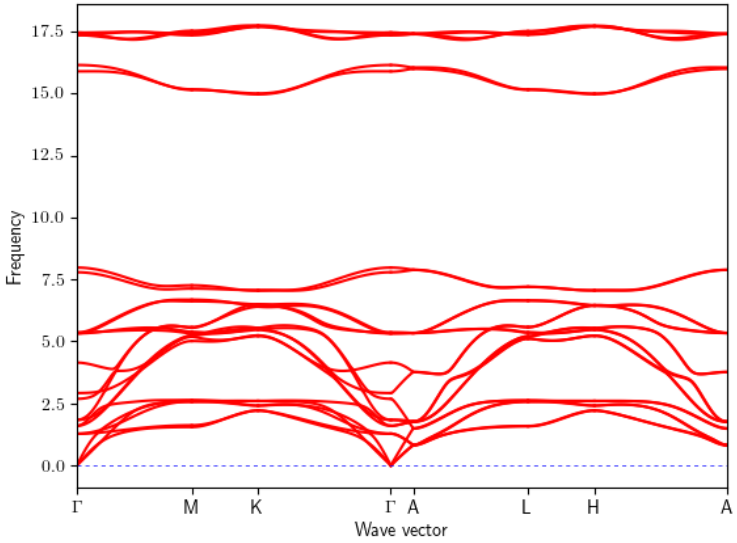

Zr_2TlN

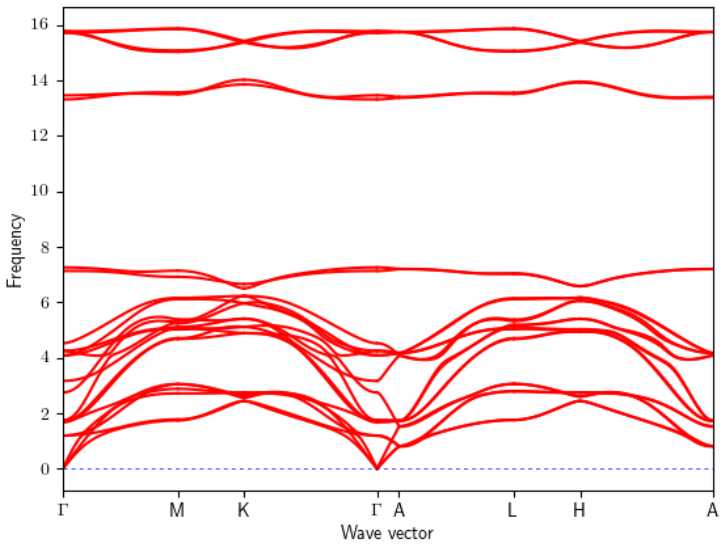

Zr_3AlC_2

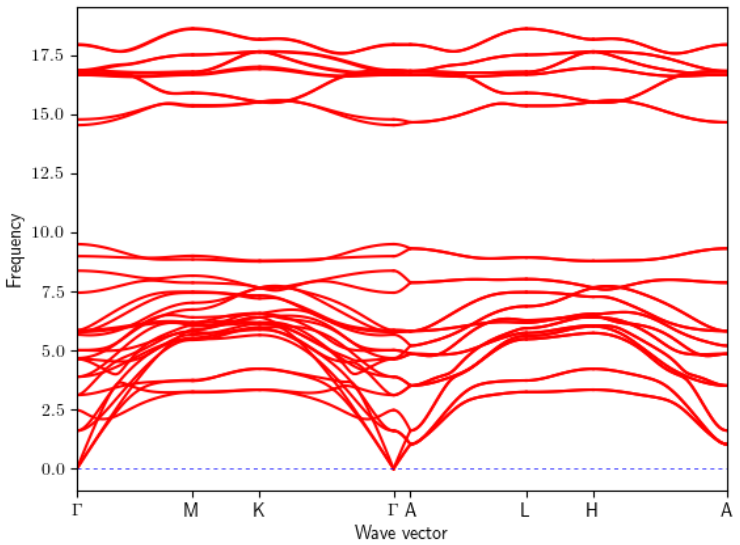

Table 1S

k: the force constant (eV/Å^2), **r**: the bond distance (Å) **FC**: summation of force constants of springs connected to a M, A, or C atom (eV/Å^2)
Bond strength (eV/bond) have been obtained using COHP analysis using PbeVasp2016 basis set except for Nb family done by default basis set.

MAX Phase	r(A-A)	k(A-A)	r(M1-A)	k(M1-A)	onding streng	r(M1-M1)	k(M1-M1)	r(M1-M2)	k(M1-M2)	k(M1-X)	onding streng	r(X-X)	k(X-X)	FC(M1)	FC(A)	FC(X)
Cr2AlC	2.845	1.225	2.666	1.704	−2.18904	2.845	1.376	2.703	2.552	8.502	−4.25926	2.845	0.33	50.97	22.557	57.783
Cr2GaC	2.872	0.976	2.649	1.618	−2.49765	2.872	0.929	2.69	2.572	7.981	−4.3525	2.872	0.034	45.531	20.775	53.94
Cr2GaN	2.9	0.906	2.671	1.397	−2.44809	2.9	0.592	2.608	1.909	6.327	−4.27616	2.9	0.761	35.449	19.492	47.339
Cr2GeC	2.939	0.867	2.609	1.608	−2.9489	2.939	0.242	2.659	2.804	7.798	−4.28059	2.939	0.326	40.196	22.433	53.649
Sc2AlC	3.287	0.133	3.156	0.887	−1.66648	3.287	1.032	3.123	2.129	4.029	−3.4269	3.287	1.028	30.56	6.412	30.45
Sc2GaC	3.296	0.258	3.097	0.806	−1.84483	3.296	1.017	3.122	2.115	3.917	−3.52164	3.296	1.049	29.776	5.59	30.227
Sc2InC	3.348	0.312	3.26	0.844	−1.74497	3.348	0.964	3.114	2.025	3.806	−3.46993	3.348	0.886	28.622	8.771	28.523
Sc2TlC	3.367	0.593	3.259	0.808	−1.82241	3.367	0.926	3.112	1.972	3.701	−3.43002	3.367	0.849	27.69	9.628	27.793
Ti2AlC	3.069	0.463	2.891	1.745	−2.01762	3.069	1.355	2.901	3.01	7.108	−3.86432	3.069	0.435	46.742	15.077	51.518
Ti2AlN	2.996	0.751	2.832	2.037	−2.07817	2.996	1.857	2.907	2.051	6.514	−3.76591	2.996	0.552	45.139	18.813	50.626
Ti2AsC	3.189	0.746	2.641	2.489	−3.30872	3.189	1.14	2.925	2.842	5.127	−3.75348	3.189	0.201	39.82	25.519	41.355
Ti2CdC	3.104	0.639	3.083	1.016	−1.71855	3.104	0.825	2.882	3.124	6.598	−3.86547	3.104	0.22	40.212	11.683	47.573
Ti2GaC	3.081	0.354	2.842	1.757	−2.27596	3.081	1.33	2.898	3.015	7.036	−3.96102	3.081	0.366	45.831	14.594	50.935
Ti2GaN	3.016	0.564	2.789	2.115	−2.36426	3.016	1.76	2.893	2.2	6.579	−3.81702	3.016	0.5	44.726	17.942	50.307
Ti2GeC	3.091	0.365	2.755	2.304	−2.73811	3.091	1.681	2.922	2.541	6.633	−3.90139	3.091	0.404	44.931	19.016	49.4
Ti2InC	3.149	1.034	3.046	1.421	−2.03394	3.149	0.858	2.867	3.081	6.795	−3.88384	3.149	0.227	42.657	17.174	47.441
Ti2InN	3.101	1.357	2.997	1.606	−2.09769	3.101	1.823	2.843	1.415	6.017	−3.74522	3.101	0.186	37.838	19.971	44.642
Ti2PbC	3.228	1.639	3.059	1.312	−2.36674	3.228	0.977	2.848	2.54	6.036	−3.77412	3.228	0.047	36.202	20.543	41.906
Ti2PC	3.182	0.568	2.513	3.342	−3.39497	3.182	1.327	2.966	2.917	4.396	−3.63204	3.182	0.439	41.091	30.756	39.724
Ti2SC	3.205	1.236	2.511	3.409	−3.23625	3.205	0.241	2.901	2.816	5.942	−3.65926	3.205	0.213	43.523	34.839	45.014
Ti2SiC	3.053	0.002	2.691	2.781	−2.68386	3.053	1.889	2.946	2.578	6.768	−3.80834	3.053	0.547	48.296	19.366	51.315
Ti2SnC	3.177	1.258	2.973	1.694	−2.44509	3.177	1.197	2.879	2.588	6.213	−3.81244	3.177	0.158	39.995	21.586	44.679
Ti2TlC	3.175	1.321	3.064	1.281	−2.0926	3.175	0.84	2.858	3.11	6.598	−3.82041	3.175	0.155	40.701	17.438	45.923
V2AlC	2.908	1.027	2.736	2.056	−2.19446	2.908	1.914	2.795	2.409	8.235	−4.09971	2.908	0.413	51.943	21.855	59.168
V2AsC	3.105	1.003	2.551	2.941	−3.52313	3.105	0.263	2.741	2.597	6.665	−3.95988	3.105	0.128	39.742	32.674	47.374
V2GaC	2.937	0.699	2.708	2.034	−2.50438	2.937	1.534	2.771	2.835	8.223	−4.19436	2.937	0.231	50.948	19.803	58.198
V2GaN	2.921	0.841	2.702	1.793	−2.50768	2.921	1.159	2.737	1.565	7.054	−4.03227	2.921	0.567	41.451	20.107	48.01
V2GeC	3.005	0.719	2.637	2.271	−3.02071	3.005	1.054	2.752	2.501	7.616	−4.10165	3.005	0.359	44.669	24.124	52.022
V2PC	3.069	0.625	2.424	4.134	−3.52391	3.069	0.105	2.774	3.043	6.576	−3.87818	3.069	0.297	45.336	38.957	49.711
V2SiC	2.952	0.343	2.543	3.098	−2.99064	2.952	1.674	2.805	2.308	7.617	−4.02850	2.952	0.147	50.602	25.993	54.431
Mo2GaC	3.067	0.475	2.764	1.784	−2.67281	3.067	0.642	2.933	2.027	6.939	−4.40586	3.067	0.159	42.877	19.247	46.103
Nb2AsC	3.345	0.736	2.692	3.448	−2.63683	3.345	0.383	2.983	3.361	5.821	−3.44423	3.345	0.064	42.917	33.512	40.67
Nb2GaC	3.159	0.318	2.848	2.199	−1.82843	3.159	2.205	3.05	2.65	6.918	−3.69612	3.159	0.005	50.502	17.52	48.56
Nb2InC	3.205	1.023	3.058	1.76	−1.50984	3.205	1.711	3.02	3.073	6.479	−3.63596	3.205	0.149	46.239	18.884	45.318
Nb2PC	3.31	0.538	2.59	3.827	−2.659	3.31	0.434	3.014	3.523	5.575	−3.31057	3.31	0.056	45.747	36.147	41.902
Nb2SC	3.317	0.764	2.638	2.213	−2.22507	3.317	0.088	2.945	3.644	6.134	−3.37407	3.317	0.143	38.282	27.112	42.841
Nb2SnC	3.275	1.057	3	1.845	−1.82071	3.275	0.948	2.98	3.282	6.412	−3.54825	3.275	0.493	42.456	22.211	41.843
Zr2AlC	3.331	0.011	3.064	1.706	−2.07628	3.331	1.647	3.185	3.217	5.632	−3.79338	3.331	0.256	43.626	11.852	41.725

Continue of Table 1S

MAX Phase	r(A-A)	k(A-A)	r(M1-A)	k(M1-A)	onding streng	r(M1-M1)	k(M1-M1)	r(M1-M2)	k(M1-M2)	k(M1-X)	onding streng	r(X-X)	k(X-X)	FC(M1)	FC(A)	FC(X)
Zr2AlN	3.258	0.131	2.993	2.122	−2.16649	3.258	2.086	3.179	2.21	5.041	−3.69334	3.258	0.172	41.963	15.047	39.488
Zr2BiC	3.477	0.983	3.16	1.448	−2.69841	3.477	1.029	3.125	2.966	5.019	−3.70765	3.477	0.108	36.256	18.344	35.309
Zr2InC	3.376	0.511	3.202	1.469	−2.05708	3.376	1.346	3.153	3.479	5.641	−3.84592	3.376	0.117	42.055	13.475	40.623
Zr2InN	3.305	0.722	3.14	1.754	−2.134	3.305	1.7	3.148	2.254	4.885	−3.69755	3.305	0.13	38.546	16.327	37.17
Zr2PbC	3.417	0.86	3.191	1.571	−2.43959	3.417	1.358	3.148	2.856	5.364	−3.77725	3.417	0.026	38.492	16.658	38.082
Zr2SC	3.431	0.8	2.695	3.117	−3.17825	3.431	0.767	3.163	2.998	5.421	−3.65059	3.431	0.028	43.731	29.266	39.773
Zr2SnC	3.381	0.682	3.123	1.855	−2.4956	3.381	1.761	3.177	2.733	5.33	−3.78514	3.381	0.183	40.914	17.769	39.306
Zr2TlC	3.392	0.568	3.215	1.366	−2.1178	3.392	1.18	3.143	3.33	5.748	−3.82943	3.392	0.073	41.106	13.693	40.182
Zr2TlN	3.322	0.861	3.157	1.646	−2.1942	3.322	1.643	3.135	2.152	4.879	−3.6936	3.322	0.056	36.856	16.38	36.312
Hf2AlC	3.273	0.11	3.017	1.879	−2.26667	3.273	1.683	3.127	3.309	6.164	−4.07078	3.273	0.448	46.861	13.999	47.038
Hf2AlN	3.192	0.284	2.947	2.311	−2.34592	3.192	2.311	3.148	2.145	5.241	−3.94467	3.192	0.248	44.368	17.288	42.212
Hf2InC	3.324	0.68	3.161	1.59	−2.27445	3.324	1.356	3.092	3.729	6.126	−4.17183	3.324	0.255	44.911	15.64	45.447
Hf2PbC	3.377	1.027	3.156	1.642	−2.6474	3.377	1.238	3.079	3.167	5.798	−4.08593	3.377	0.117	40.731	18.518	41.947
Hf2SC	3.378	0.913	2.663	3.206	−3.3959	3.378	0.804	3.094	3.138	5.971	−3.88199	3.378	0.105	46.386	31.323	44.56
Hf2SnC	3.342	0.725	3.082	1.975	−2.73194	3.342	1.566	3.106	2.961	5.742	−4.10642	3.342	0.314	42.818	19.217	43.319
Hf2SnN	3.262	1.081	3.057	1.98	−2.05246	3.262	1.513	3.116	2.182	4.65	−3.34131	3.262	0.198	37.466	21.213	35.561
Hf2TlC	3.342	0.89	3.174	1.507	−2.31834	3.342	1.241	3.081	3.715	6.172	−4.09257	3.342	0.165	43.945	16.117	44.767
Ta2AlC	3.094	0.565	2.861	2.261	−2.48819	3.094	2.542	3.078	1.888	7.895	−4.3833	3.094	0.244	55.019	20.596	57.183
Ta2GaC	3.122	0.409	2.83	2.32	−2.80341	3.122	2.378	3.05	2.332	7.814	−4.51404	3.122	0.025	52.729	19.464	55.684
Ti3AlC2	3.083	0.45	2.9	1.766	−2.01814	3.083	1.45	2.966	2.654	8.318	−4.23572	3.083	0.52	49.175	14.708	49.514
Ti3AuC2	3.086	0.563	2.897	0.882	−2.1332	3.086	1.259	2.974	2.559	7.405	−4.23797	3.086	0.638	42.706	12.108	47.647
Ti3GeC2	3.1	0.344	2.766	2.204	−2.70938	3.1	1.639	2.96893	2.548	7.815	−4.27421	3.1	0.416	48.448	18.867	48.641
Ti3IrC2	3.025	0.732	2.731	1.548	−2.63087	3.025	1.566	3.010	2.211	7.404	−4.15949	3.025	0.851	46.117	19.702	50.703
Ti3SiC2	3.076	0.05	2.702	2.646	−2.68617	3.076	1.822	2.982	2.5	7.693	−4.10901	3.076	0.517	50.223	18.786	49.697
Ti3SnC2	3.151	1.48	2.978	1.686	−2.40074	3.151	1.354	2.952	2.522	7.674	−4.24577	3.151	0.284	45.117	22.225	45.549
V3AlC2	2.919	1.034	2.744	1.953	−2.18294	2.919	2.243	2.858	1.512	8.504	−4.38841	2.919	0.737	52.601	20.894	55.76
V3SiC2	2.929	0.166	2.572	2.546	−2.92062	2.929	1.628	2.874	1.401	7.157	−4.25027	2.929	0.511	44.785	22.358	51.296
Zr3AlC2	3.348	0.001	3.068	1.758	−2.08301	3.348	1.702	3.246	2.891	6.739	−4.21975	3.348	0.359	46.019	11.886	40.511
Nb3SiC2	3.177	0.043	2.698	2.591	−2.92458	3.177	1.7	3.139	1.387	5.155	−4.44613	3.177	0.241	39.718	22.045	41.391
Ta3AlC2	3.1	0.507	2.861	2.296	−2.48598	3.1	2.725	3.140	0.907	7.607	−4.11931	3.1	0.484	55.52	20.536	55.922
Ti4AlN3	2.998	0.783	2.832	2.031	−2.08196	2.998	2.177	2.931	1.391	7.048	−3.88905	2.998	0.799	48.502	19.08	51.258
Ti4GaC3	3.092	0.348	2.841	1.87	−2.28241	3.092	1.522	2.995	2.456	8.411	−4.43242	3.092	0.542	48.883	14.668	47.563
Ti4GeC3	3.098	0.351	2.762	2.279	−2.72256	3.098	1.647	2.997	2.511	7.8	−4.34525	3.098	0.493	48.452	19.118	46.894
Ti4SiC3	3.08	0.068	2.700	2.7		3.08	1.789	3.006	2.471	7.622		3.08	0.577	49.771	18.801	47.71
V4AlC3	2.919	1.054	2.749	2.008	−2.18204	2.919	2.207	2.835	1.766	9.305	−4.4046	2.919	0.729	55.815	20.866	58.123
Nb4AlC3	3.161	0.297	2.902	1.995		3.161	2.334	3.083	2.26	7.372		3.161	0.171	53.323	16.68	48.319
Ta4AlC3	3.138	0.376	2.885	2.044	−2.45916	3.138	2.231	3.067	2.105	7.979	−4.10015	3.138	0.143	53.959	18.618	55.066
Nb5AlC4	3.149	0.338	2.917	1.949		3.149	2.731	3.122	0.902	6.425		3.149	0.379	48.966	15.724	45.336
Ti5AlC4	3.079	0.435	2.927	1.415	−1.93954	3.079	1.332	3.009	2.567	8.008	−4.40264	3.079	0.473	46.434	12.395	45.731
Mo2ScAlC2	3.055	0.616	2.775	2.155	−2.424	3.055	3.042	3.159	1.198	6.132	−4.863	3.055	1.169	45.17	20.251	44.822
Mo2TiAlC2	3.003	0.708	2.785	1.953	−2.38687	3.003	2.71	3.047	0.853	7.843	−4.69234	3.003	0.625	49.797	20.086	52.324
Cr2TiAlC2	2.908	0.927	2.681	1.691	−2.20154	2.908	1.39	2.898	1.362	8.105	−4.60564	2.908	0.638	44.253	20.124	53.691
Mo2Ti2AlC3	3.025	0.649	2.782	2.062	−2.40998	3.025	2.566	3.034	1.478	8.187	−4.73012	3.025	0.524	51.522	20.094	52.379

Table 2S: Sorted data for FC(M), FC(A), FC(X) (eV/Å^2), and exfoliation energy (eV/Å^2)

MAX Phase	FC(M)			MAX Phase	FC(A)			MAX Phase	FC(X)			MAX Phase	Exfoliation energy		
V4AlC3	55.815	Ti2GaN	44.726	Sc2GaC	5.59	Ti4GeC3	19.118	Cr2AlC	57.783	Ti4GeC3	46.894	Sc2AlC	0.086	Ta5AlC4	0.177
Ta3AlC2	55.52	V2GeC	44.669	Sc2AlC	6.412	Hf2SnC	19.217	V2AlC	59.168	Mo2GaC	46.103	Sc2TlC	0.094	Ti3SiC2	0.181
Ta2AlC	55.019	Hf2AlN	44.368	Sc2InC	8.771	Mo2GaC	19.247	V2GaC	58.198	Ti2TlC	45.923	Sc2InC	0.105	Ti4SiC3	0.181
Ta4AlC3	53.959	Cr2TiAlC2	44.253	Sc2TlC	9.628	Ti2SiC	19.366	V4AlC3	58.123	Ti5AlC4	45.731	Sc2GaC	0.105	Cr2TiAlC2	0.184
Nb4AlC3	53.323	Hf2TlC	43.945	Ti2CdC	11.683	Ta2GaC	19.464	Ta2AlC	57.183	Ti3SnC2	45.549	Ti2PbC	0.119	Nb2GaC	0.185
Ta2GaC	52.729	Zr2SC	43.731	Zr2AlC	11.852	Cr2GaN	19.492	Ta3AlC2	55.922	Hf2InC	45.447	Ti2CdC	0.121	Nb2AlC	0.185
V3AlC2	52.601	Zr2AlC	43.626	Zr3AlC2	11.886	Ti3IrC2	19.702	V3AlC2	55.76	Nb5AlC4	45.336	Ti2TlC	0.122	Ti3GeC2	0.185
V2AlC	51.943	Ti2SC	43.523	Ti3AuC2	12.108	V2GaC	19.803	Ta2GaC	55.684	Nb2InC	45.318	Zr2TlC	0.122	Nb2AsC	0.186
Nb2AlC	51.706	Nb2AsC	42.917	Ti5AlC4	12.395	Ti2InN	19.971	Ta4AlC3	55.066	Ti2SC	45.014	Zr2BiC	0.123	V2GeC	0.186
Mo2Ti2AlC3	51.522	Mo2GaC	42.877	Zr2InC	13.475	Mo2TiAlC2	20.086	V2SiC	54.431	Mo2ScAlC2	44.822	Hf2PbC	0.125	V2AsC	0.186
Cr2AlC	50.97	Hf2SnC	42.818	Zr2TlC	13.693	Mo2Ti2AlC3	20.094	Cr2GaC	53.94	Hf2TlC	44.767	Hf2TlC	0.126	Ti4GeC3	0.186
V2GaC	50.948	Ti3AuC2	42.706	Hf2AlC	13.999	V2GaN	20.107	Cr2TiAlC2	53.691	Ti2SnC	44.679	Zr2TlN	0.128	Ta2GaC	0.187
V2SiC	50.602	Ti2InC	42.657	Ti2GaC	14.594	Cr2TiAlC2	20.124	Cr2GeC	53.649	Ti2InN	44.642	Zr2PbC	0.129	Ti2SiC	0.188
Nb2GaC	50.502	Nb2SnC	42.456	Ti4GaC3	14.668	Mo2ScAlC2	20.251	Mo2Ti2AlC3	52.379	Hf2SC	44.56	Zr3AlC2	0.131	Cr2GaN	0.189
Ti3SiC2	50.223	Zr2InC	42.055	Ti3AlC2	14.708	Ta3AlC2	20.536	Mo2TiAlC2	52.324	Hf2SnC	43.319	Zr2AlC	0.133	Ti2GeC	0.189
Mo2TiAlC2	49.797	Zr2AlN	41.963	Zr2AlN	15.047	Ti2PbC	20.543	V2GeC	52.022	Nb2SC	42.841	Zr2InC	0.139	V3SiC2	0.190
Ti4SiC3	49.771	V2GaN	41.451	Ti2AlC	15.077	Ta2AlC	20.596	Ti2AlC	51.518	Hf2AlN	42.212	Hf2SnC	0.144	Ti2AlN	0.190
Ti3AlC2	49.175	Zr2TlC	41.106	Hf2InC	15.64	Cr2GaC	20.775	Ti2SiC	51.315	Hf2PbC	41.947	Ti5AlC4	0.145	Mo2GaC	0.191
Nb5AlC4	48.966	Ti2PC	41.091	Nb5AlC4	15.724	V4AlC3	20.866	V3SiC2	51.296	Ti2PbC	41.906	Ti3AuC2	0.146	Ta2AlC	0.192
Ti4GaC3	48.883	Zr2SnC	40.914	Hf2TlC	16.117	V3AlC2	20.894	Ti4AlN3	51.258	Nb2PC	41.902	Hf2InC	0.148	Ti4AlN3	0.193
Ti4AlN3	48.502	Hf2PbC	40.731	Zr2InN	16.327	Hf2SnN	21.213	Ti2GaC	50.935	Nb2SnC	41.843	Ti2InC	0.148	Ti2AsC	0.195
Ti4GeC3	48.452	Ti2TlC	40.701	Zr2TlN	16.38	Ti2SnC	21.586	Ti3IrC2	50.703	Zr2AlC	41.725	Hf2AlC	0.150	Mo2TiAlC2	0.196
Ti3GeC2	48.448	Ti2CdC	40.212	Zr2PbC	16.658	V2AlC	21.855	Ti2AlN	50.626	Nb3SiC2	41.391	Hf2SnN	0.150	Ta4AlC3	0.197
Ti2SiC	48.296	Cr2GeC	40.196	Nb4AlC3	16.68	Nb3SiC2	22.045	Ti2GaN	50.307	Ti2AsC	41.355	Zr2InN	0.151	Cr2GaC	0.197
Hf2AlC	46.861	Ti2SnC	39.995	Ti2InC	17.174	Nb2SnC	22.211	V2PC	49.711	Nb2AsC	40.67	Nb2SnC	0.152	Ti2GaN	0.197
Ti2AlC	46.742	Ti2AsC	39.82	Hf2AlN	17.288	Ti3SnC2	22.225	Ti3SiC2	49.697	Zr2InC	40.623	Ti2InN	0.153	V3AlC2	0.199
Ti5AlC4	46.434	V2AsC	39.742	Ti2TlC	17.438	V3SiC2	22.358	Ti3AlC2	49.514	Zr3AlC2	40.511	Nb2InC	0.155	Mo2Ti2AlC3	0.199
Hf2SC	46.386	Nb3SiC2	39.718	Nb2GaC	17.52	Cr2GeC	22.433	Ti2GeC	49.4	Zr2TlC	40.182	Zr2AlN	0.158	V4AlC3	0.201
Nb2InC	46.239	Zr2InN	38.546	Zr2SnC	17.769	Cr2AlC	22.557	Nb2AlC	49.187	Zr2SC	39.773	Ti3AlC2	0.158	V2GaC	0.202
Ti3IrC2	46.117	Zr2PbC	38.492	Ti2GaN	17.942	V2GeC	24.124	Ti3GeC2	48.641	Ti2PC	39.724	Zr2SnC	0.158	V2SiC	0.205
Zr3AlC2	46.019	Nb2SC	38.282	Nb2AlC	18.205	Ti2AsC	25.519	Nb2GaC	48.56	Zr2AlN	39.488	Ti2SnC	0.160	V2AlC	0.205
Ti2GaC	45.831	Ti2InN	37.838	Zr2BiC	18.344	V2SiC	25.993	Nb4AlC3	48.319	Zr2SnC	39.306	Ti3SnC2	0.161	Ta3AlC2	0.206
Nb2PC	45.747	Hf2SnN	37.466	Hf2PbC	18.518	Nb2SC	27.112	V2GaN	48.01	Zr2PbC	38.082	Ti2AlC	0.164	Cr2AlC	0.211
Cr2GaC	45.531	Zr2TlN	36.856	Ta4AlC3	18.618	Zr2SC	29.266	Ti4SiC3	47.71	Zr2InN	37.17	Nb5AlC4	0.165	V2GaN	0.214
V2PC	45.336	Zr2BiC	36.256	Ti3SiC2	18.786	Ti2PC	30.756	Ti3AuC2	47.647	Zr2TlN	36.312	Ti3IrC2	0.169	Nb2PC	0.219
Mo2ScAlC2	45.17	Ti2PbC	36.202	Ti4SiC3	18.801	Hf2SC	31.323	Ti2CdC	47.573	Hf2SnN	35.561	Hf2AlN	0.169	Nb2SC	0.220
Ti2AlN	45.139	Cr2GaN	35.449	Ti2AlN	18.813	V2AsC	32.674	Ti4GaC3	47.563	Zr2BiC	35.309	Ti4GaC3	0.173	Ti2PC	0.220
Ti3SnC2	45.117	Sc2AlC	30.56	Ti3GeC2	18.867	Nb2AsC	33.512	Ti2InC	47.441	Sc2AlC	30.45	Cr2GeC	0.173	V2PC	0.229
Ti2GeC	44.931	Sc2GaC	29.776	Nb2InC	18.884	Ti2SC	34.839	V2AsC	47.374	Sc2GaC	30.227	Nb3SiC2	0.175	Zr2SC	0.264
Hf2InC	44.911	Sc2InC	28.622	Ti2GeC	19.016	Nb2PC	36.147	Cr2GaN	47.339	Sc2InC	28.523	Nb4AlC3	0.175	Ti2SC	0.275
V3SiC2	44.785	Sc2TlC	27.69	Ti4AlN3	19.08	V2PC	38.957	Hf2AlC	47.038	Sc2TlC	27.793	Ti2GaC	0.176	Hf2SC	0.300

Polarity of the bonds calculated through the electronegativity differences

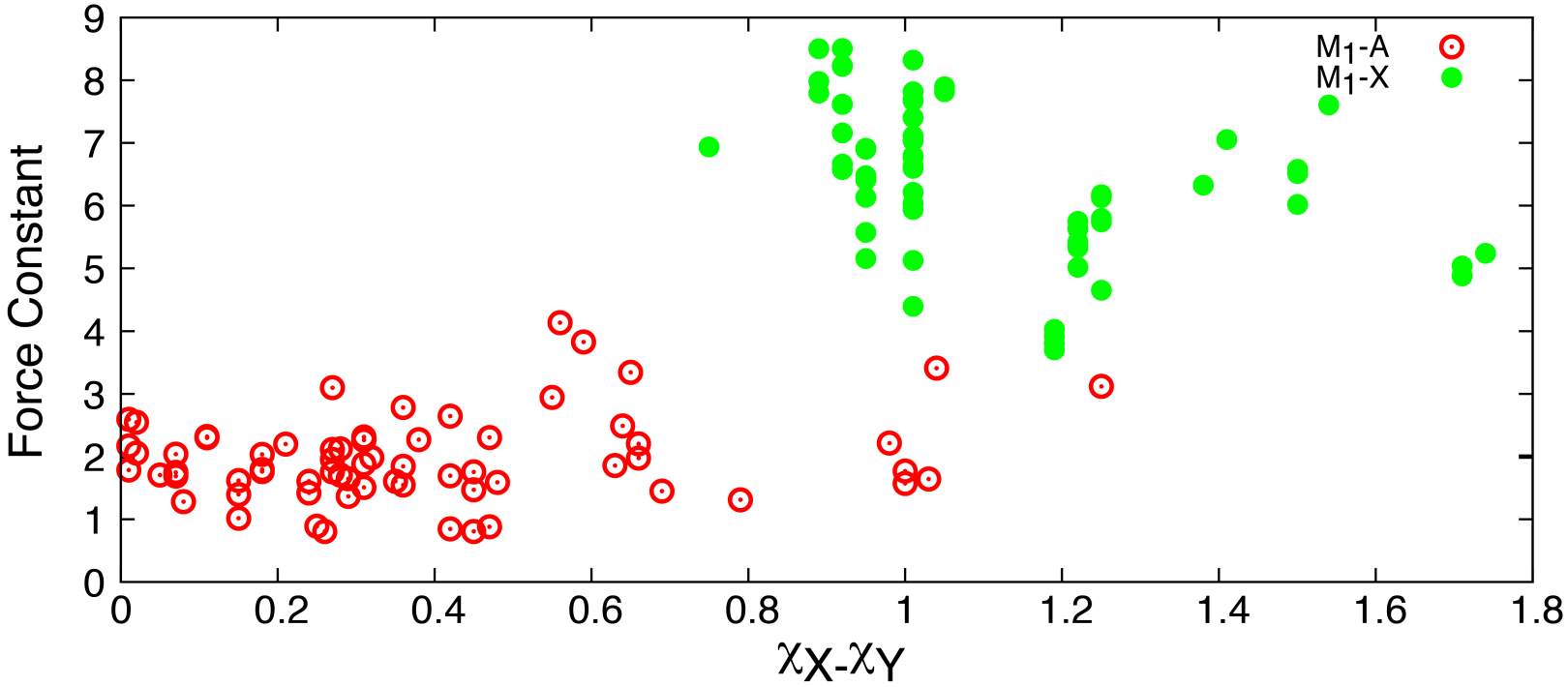

It is seen that M_1-X bonds are more polar than M_1-A bonds

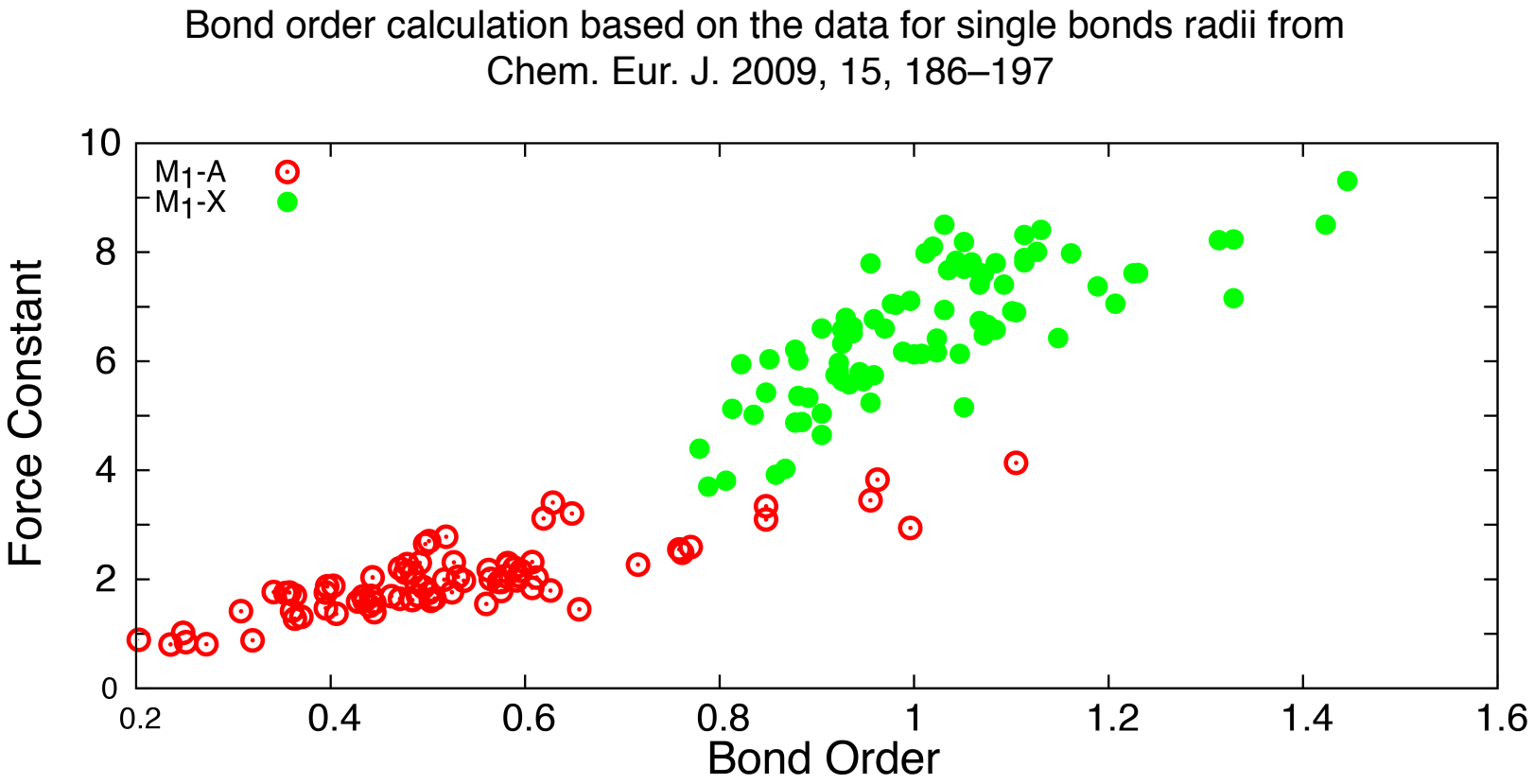

Here, we have estimated the bond order by using another set of data different from that which was used in the paper. However, the results is the same. As it was stated in the manuscript, the bond order for M_1-X bonds are larger than M_1-A bonds.

Some examples for projected density of states of positively, neutral, and negatively charged MAX phases

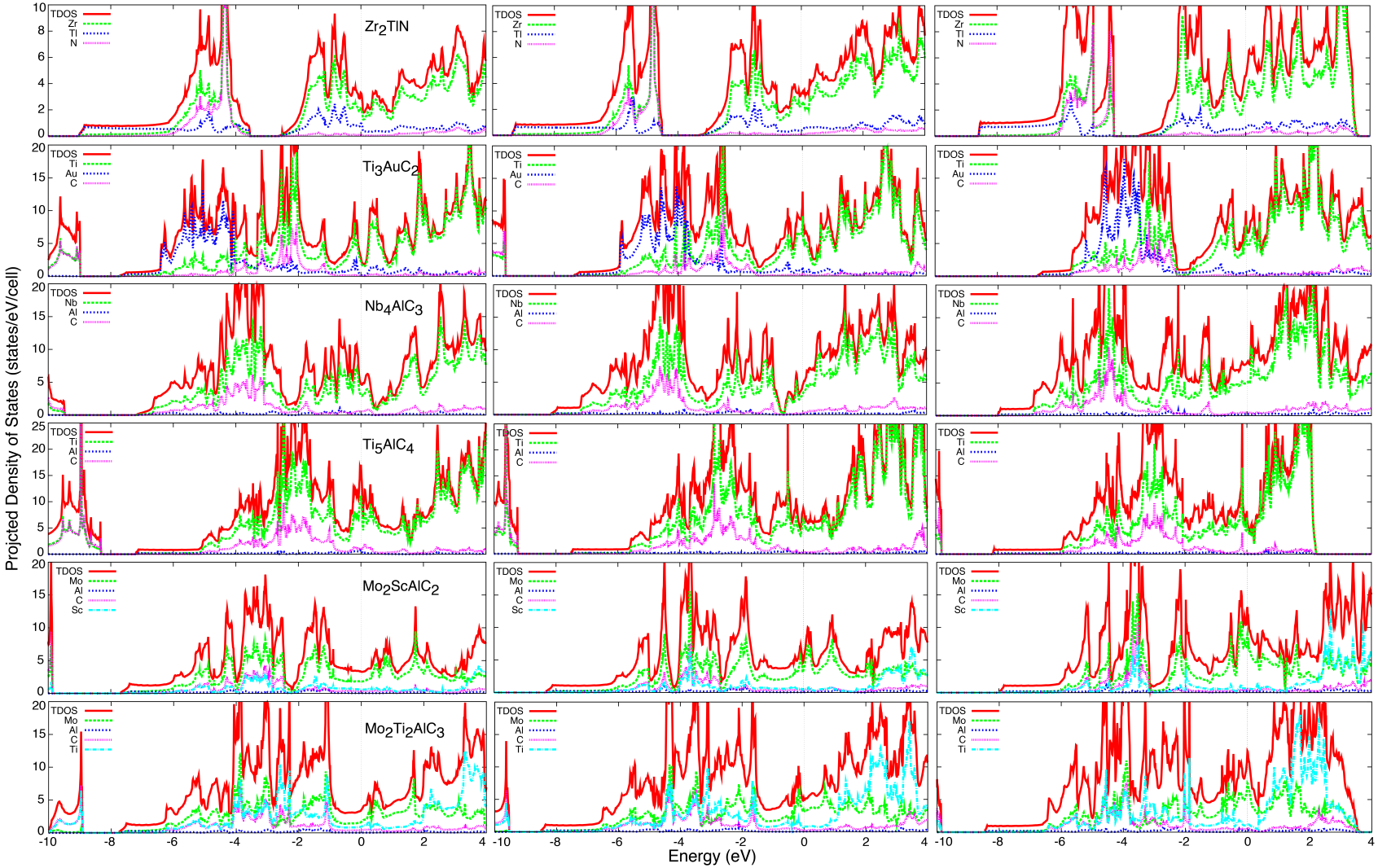

Left to right: positively, neutral, and negatively charged . The Fermi energy is at zero.

Electronic structures of neutral and charged Ti_5AlC_4

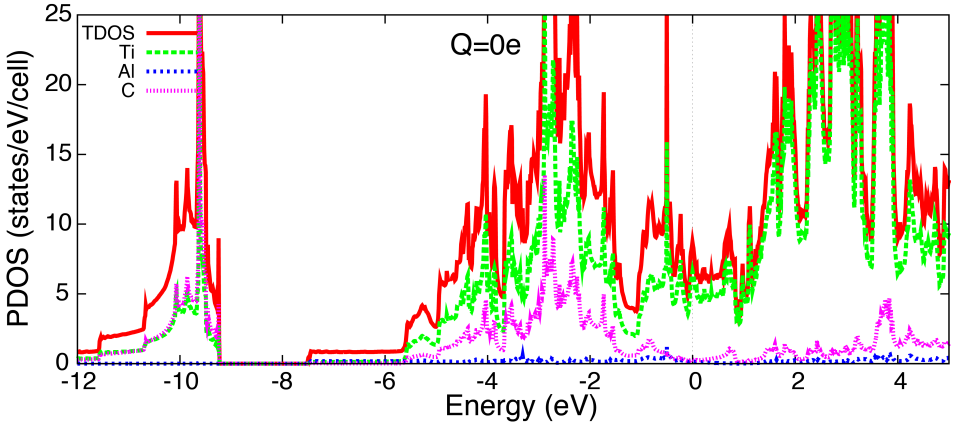

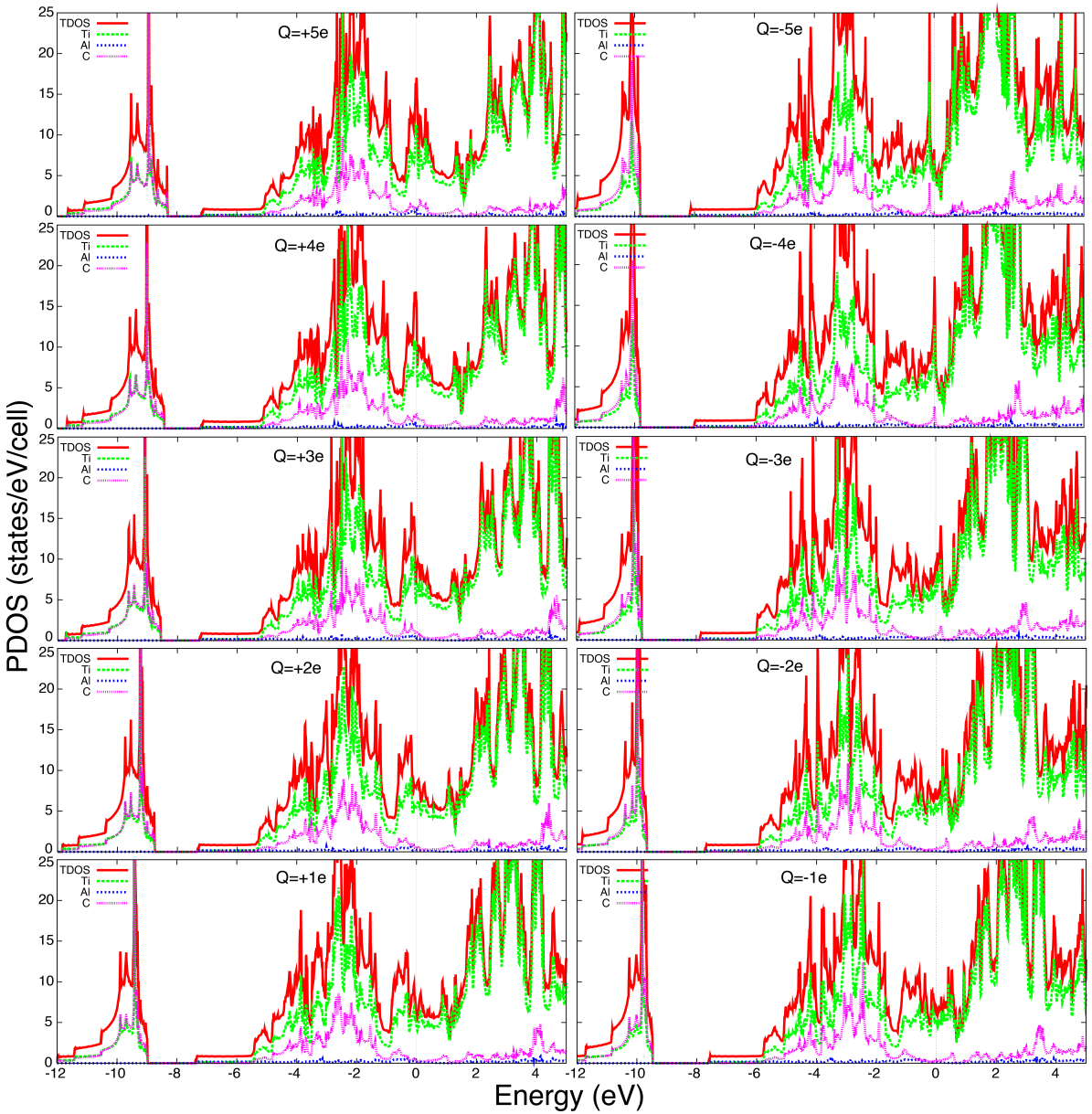

Positive (negative) Q stands for hole (electron) injection.

COHP bond analysis of neutral and charged Ti_5AlC

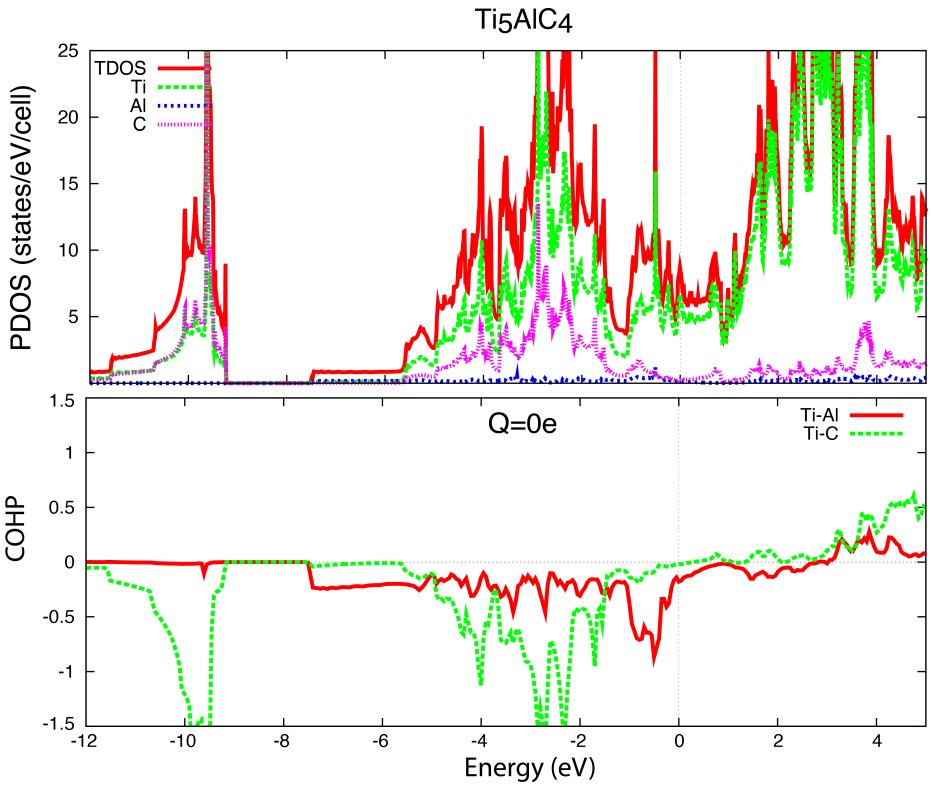

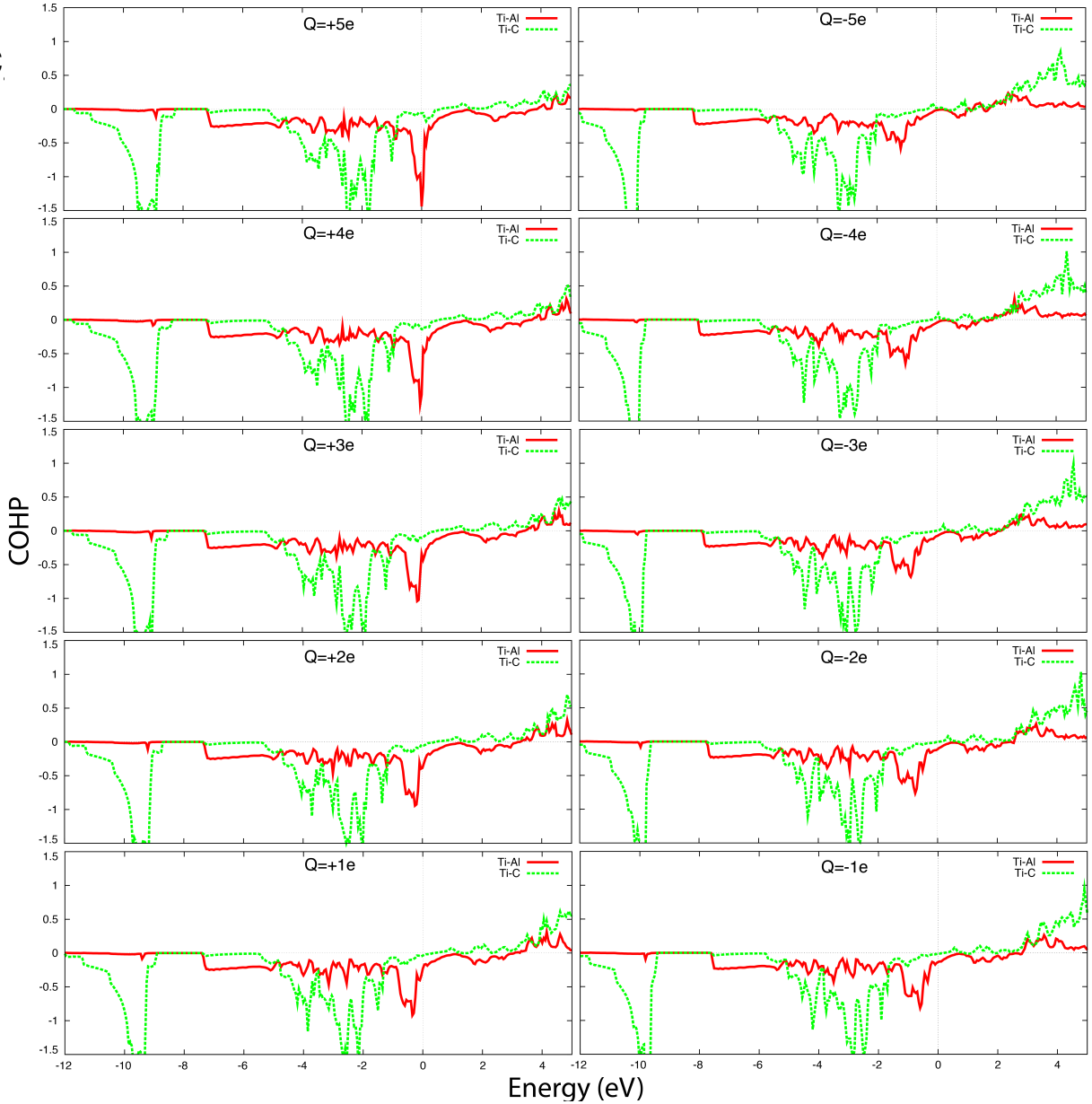

Positive (negative) Q stands for hole (electron) injection.
Positive (negative) COHP stands for antibonding (bonding) states.

Effect of hole (+) and electron (-) injection on phonon frequencies (THz) of Ti_5AlC_4

Q= +5e

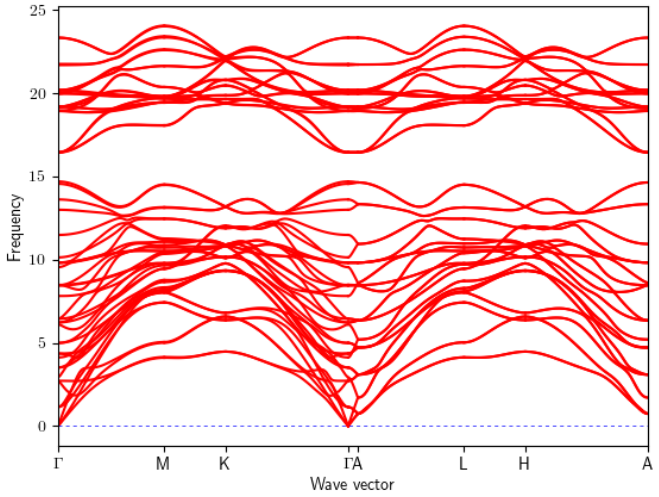

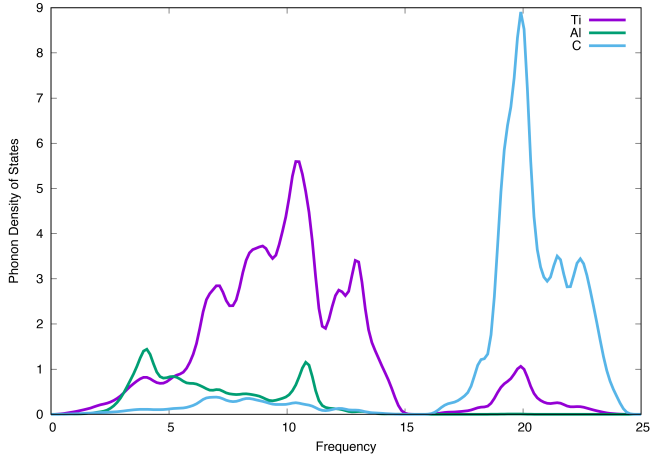

Q= +4e

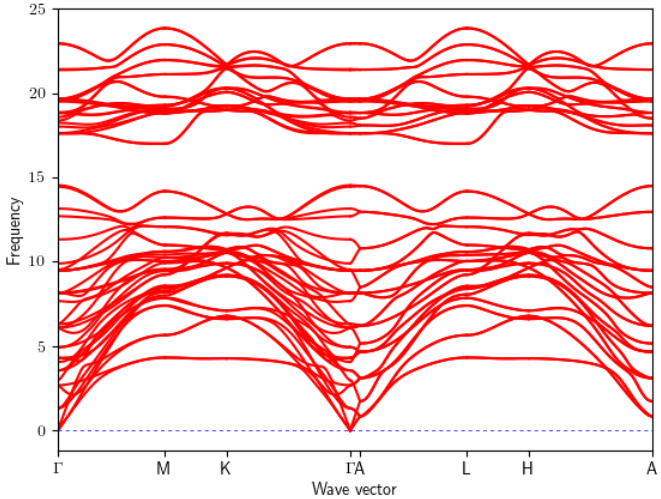

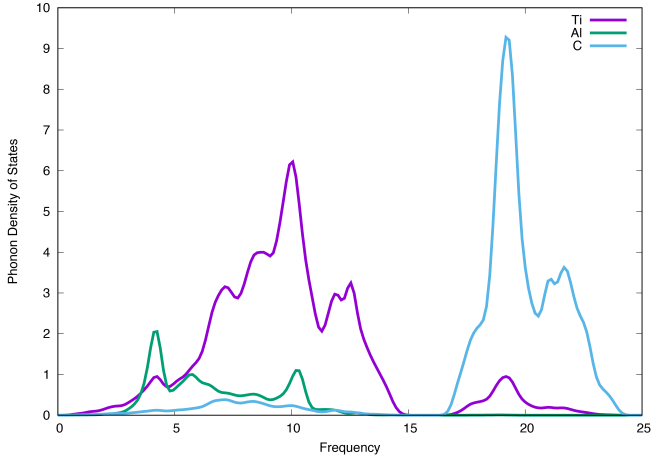

Q= +3e

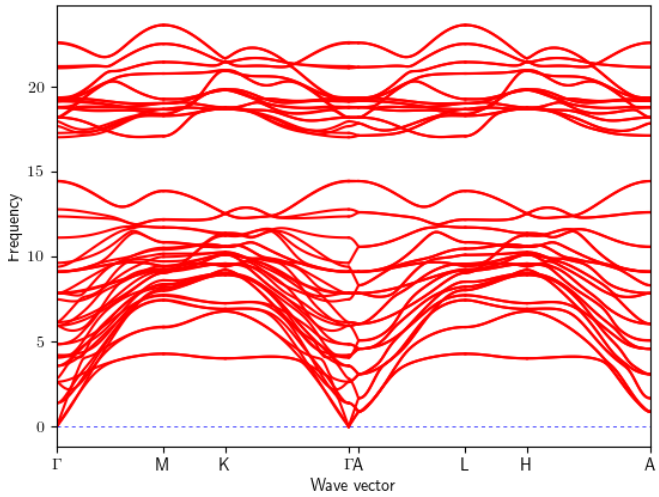

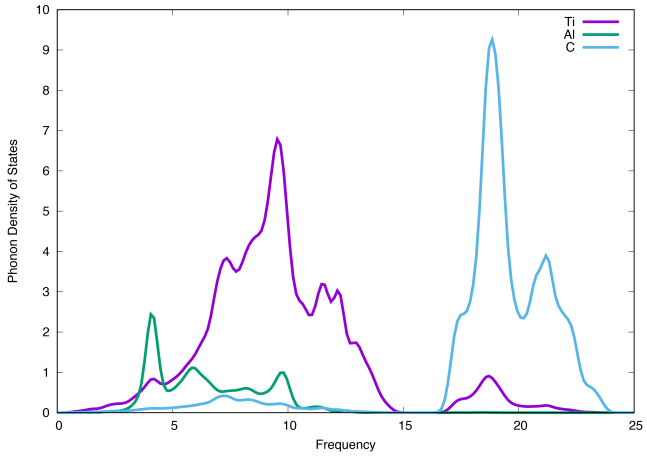

Q= +2e

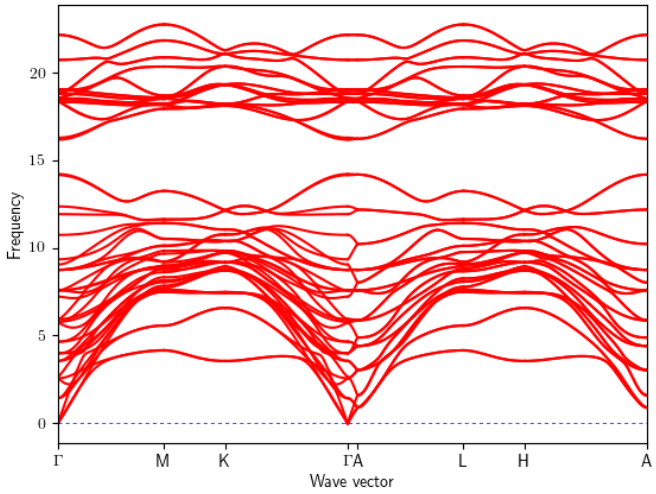
Frequency
Wave vector
Γ
M
K
ΓA
L
H
A

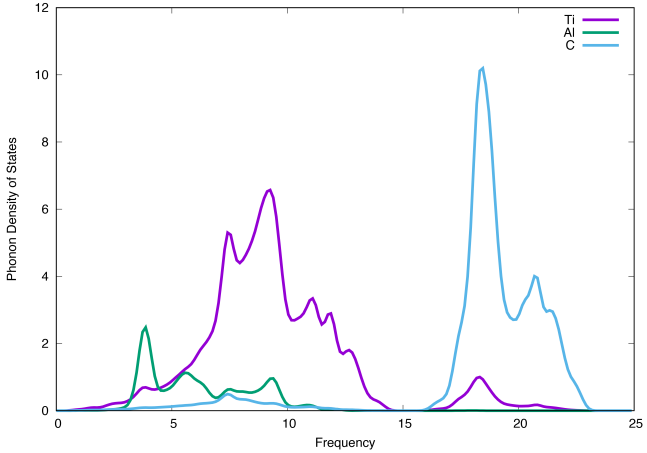
Ti
Al
C
Phonon Density of States
Frequency

Q= +1e

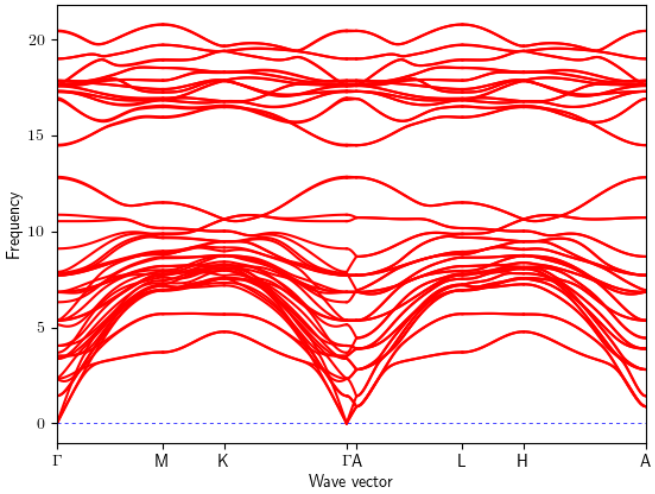
Frequency
Wave vector
Γ
M
K
ΓA
L
H
A

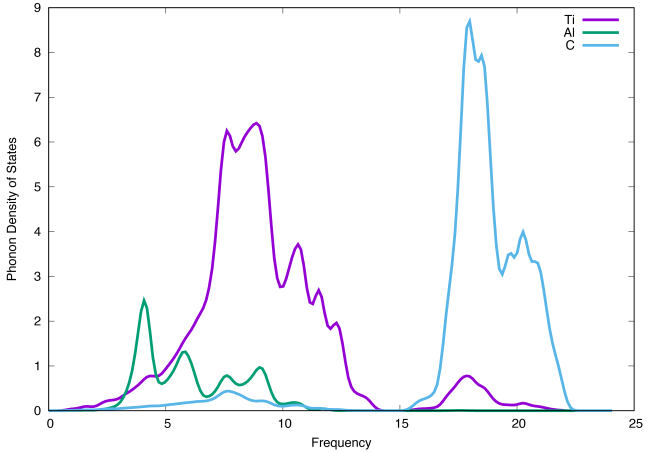
Ti
Al
C
Phonon Density of States
Frequency

Q= 0e

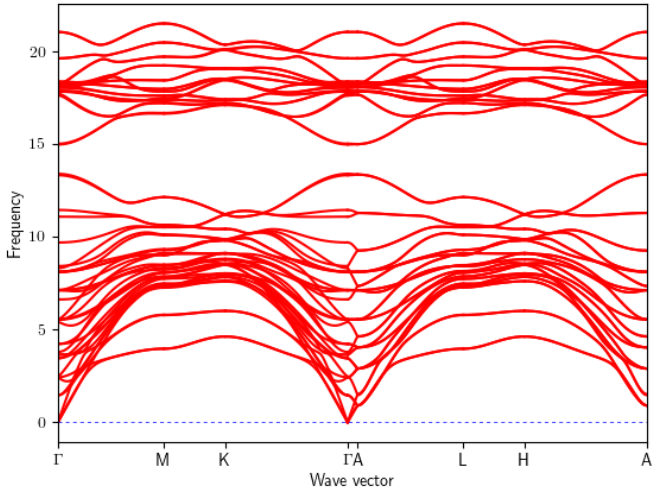
Frequency
Wave vector
Γ
M
K
ΓA
L
H
A

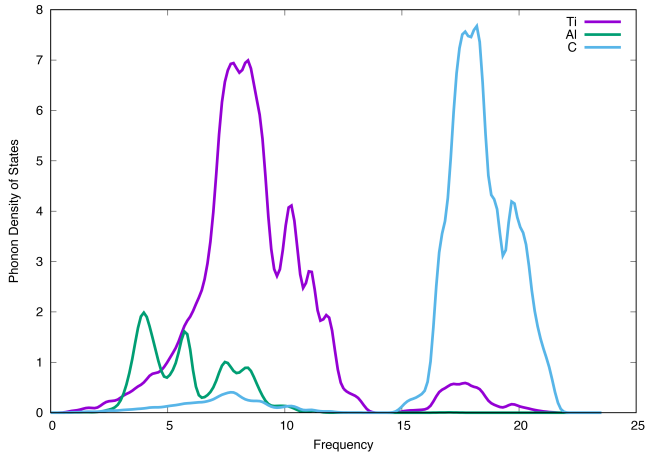
Ti
Al
C
Phonon Density of States
Frequency

Q= -1e

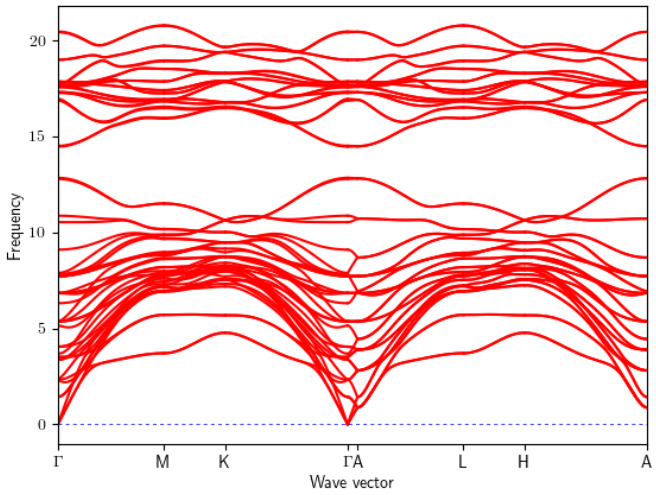
Frequency
Wave vector
Γ
M
K
ΓA
L
H
A

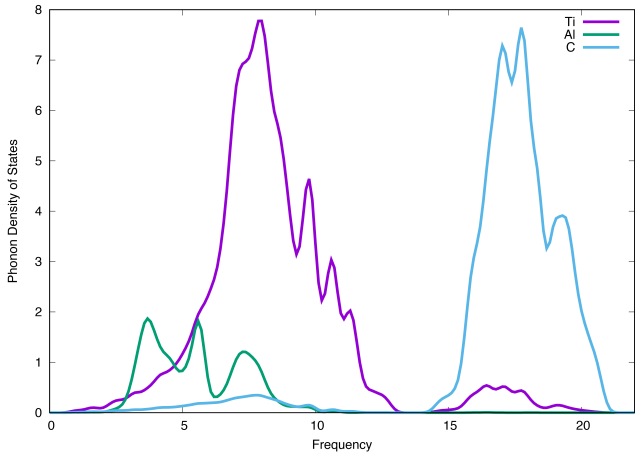
Phonon Density of States
Frequency
Ti
Al
C

Q= -2e

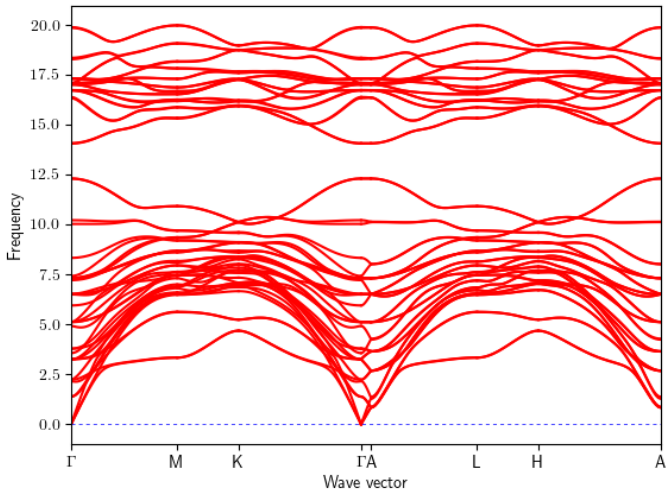
Frequency
Wave vector
Γ
M
K
ΓA
L
H
A

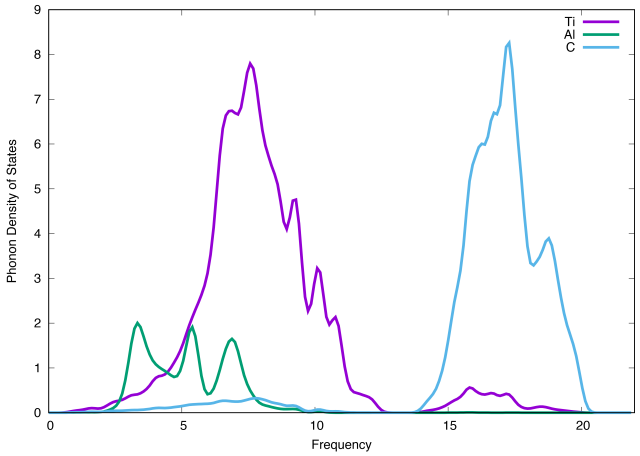
Phonon Density of States
Frequency
Ti
Al
C

Q= -3e

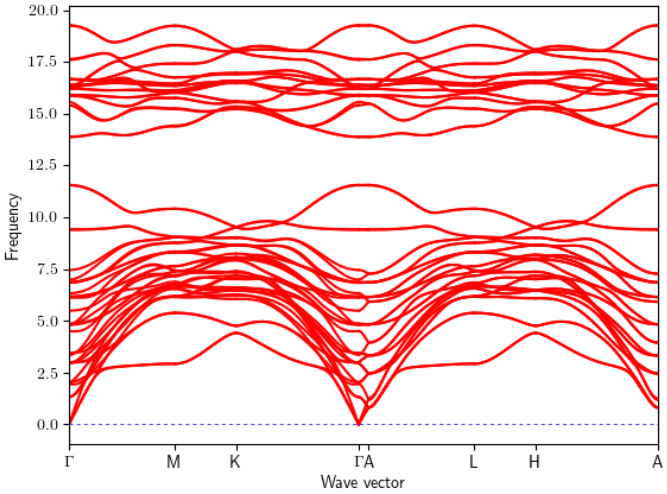
Frequency
Wave vector
Γ
M
K
ΓA
L
H
A

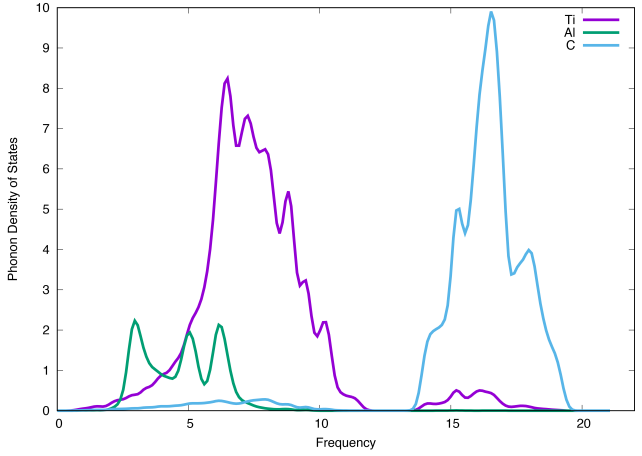
Phonon Density of States
Frequency
Ti
Al
C

Q= -4e

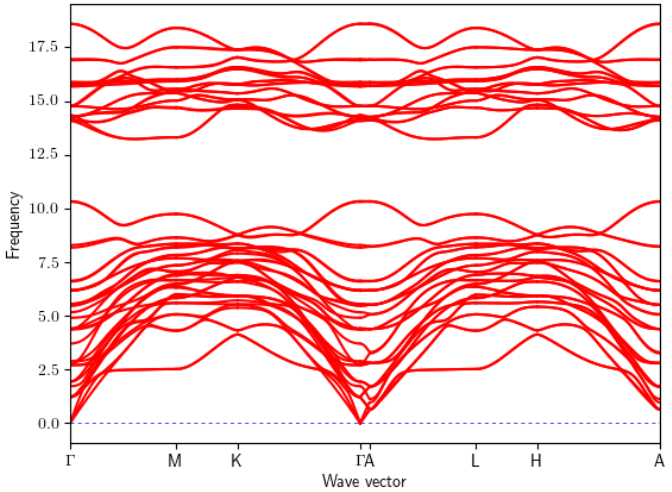
Frequency
17.5
15.0
12.5
10.0
7.5
5.0
2.5
0.0
Γ
M
K
ΓA
L
H
A
Wave vector

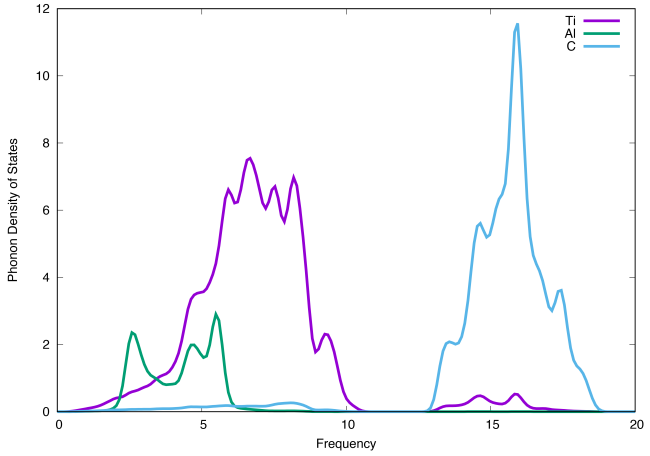
Phonon Density of States
Ti
Al
C
0
2
4
6
8
10
12
0
5
10
15
20
Frequency

Q= -5e

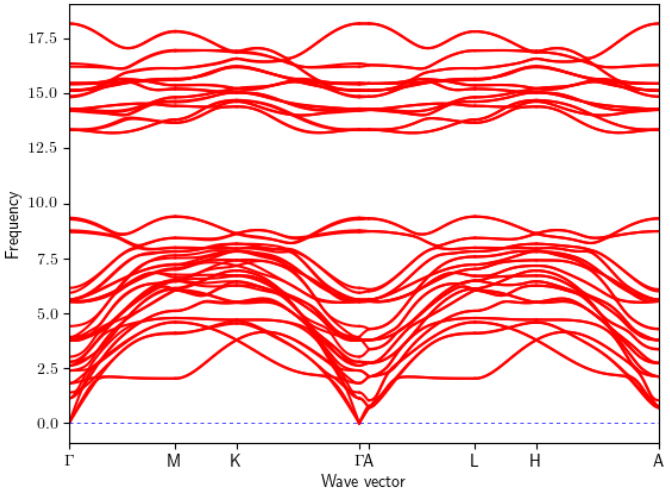
Frequency
17.5
15.0
12.5
10.0
7.5
5.0
2.5
0.0
Γ
M
K
ΓA
L
H
A
Wave vector

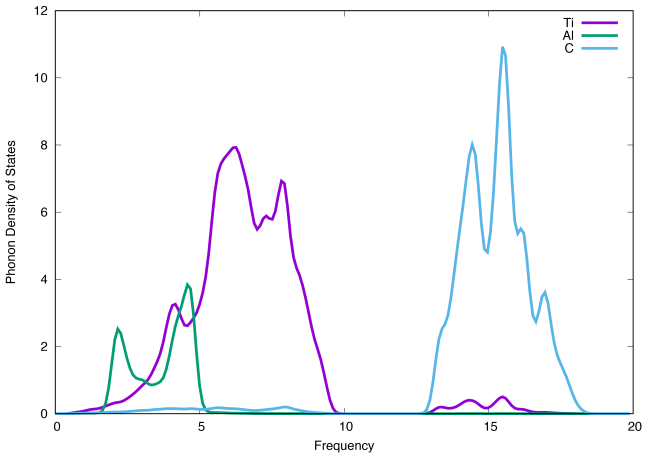
Phonon Density of States
Ti
Al
C
0
2
4
6
8
10
12
0
5
10
15
20
Frequency

RIGID BAND ANALYSIS:

In light of the assumption that the behavior of charged MAX phases can be predicted from the neutral systems using the rigid-band model, a strictly rigid-band-based ansatz was employed to compare the trends for ICOHP behavior in relation to charge injection to the trends reflected in the calculations explicitly treating charge. As above, Ti_5AlC_4 was chosen as a model system and an electronic structure and bonding analysis was performed using VASP and the Lobster code [114-116]. Then, variations in charge, reflecting electron/hole injection, were mapped to *E* in the density of states (DOS) and COHP plots, yielding shifted Fermi levels for charged systems, while the shape of the band, and by extension, DOS remained unchanged. Said energetic shift was calculated from the energy-number of valence electrons relationship from the DOS of the unperturbed system via linear regression. The resulting DOS plot is shown in Figure 1, while the COHP plots for heteroatomic (Ti–C, Ti–Al, C–Al) and homoatomic (Ti–Ti, Al–Al, C–C) interactions are given in Figure 2.

The averaged ICOHP values for a single bond of a given type as a function of the valence electron count (VEC), and by extension, charge, are shown in Figure 3. Consistent with the prior results, it is evident that the M_1–X bonds, Ti–C in this case, are significantly stronger than the M–A bonds (here, Ti–Al) among the heteroatomic bonds, while the X–A-type bond (here, C–Al) bond also shows bonding characteristics, but is negligible. In the case of the homoatomic interactions, the Al–Al bond strength is highest, with Ti–Ti and C–C showing much weaker bonding. However, if charge is injected into the system, in the rigid-bond ansatz there is *no* weakening of the Ti–Al bond. On the contrary, the ICOHP values are lower, indicating stronger bonding, with increasing negative charge, while the Ti–Al bond weakens upon injection of significant *positive* charge. The Ti–C and C–Al bonds are nearly unaffected by the variation in charge. As for the homoatomic bonds, the Al–Al bonds weaken slightly

upon introduction of high negative charge, whereas the Ti–Ti bond strength increases very faintly and C–C bonds remain essentially unaffected.

The trend for the Ti–Al bond in particular contradicts the results obtained from the models that explicitly treat the excess charge, but is easily explained in terms of the rigid-bond model: as seen in Figure 2 the COHP values for Ti–Al are negative across the entire energetic range, indicating bonding characteristics. As the electronic structure is assumed to be static in relation to small perturbations, the shape of the curve does not change upon charge injection. If the Fermi level is shifted due to an excess of electrons, the new ICOHP value will still be more negative than that of the unperturbed system; in case of electron deficiency, it will be more positive.

In contrast, for calculations which explicitly treat additional electrons, the Fermi energy surface, and thus the structure itself, change slightly, resulting in the swelling along the *c* axis described previously due to elongation of the Ti–Al bonds. As there is no structural change here, the atom distances (and thus, bond lengths) remain of fixed length and all differences in bonding characteristics reflect the small perturbation to the electronic structure from the variation in electron count.

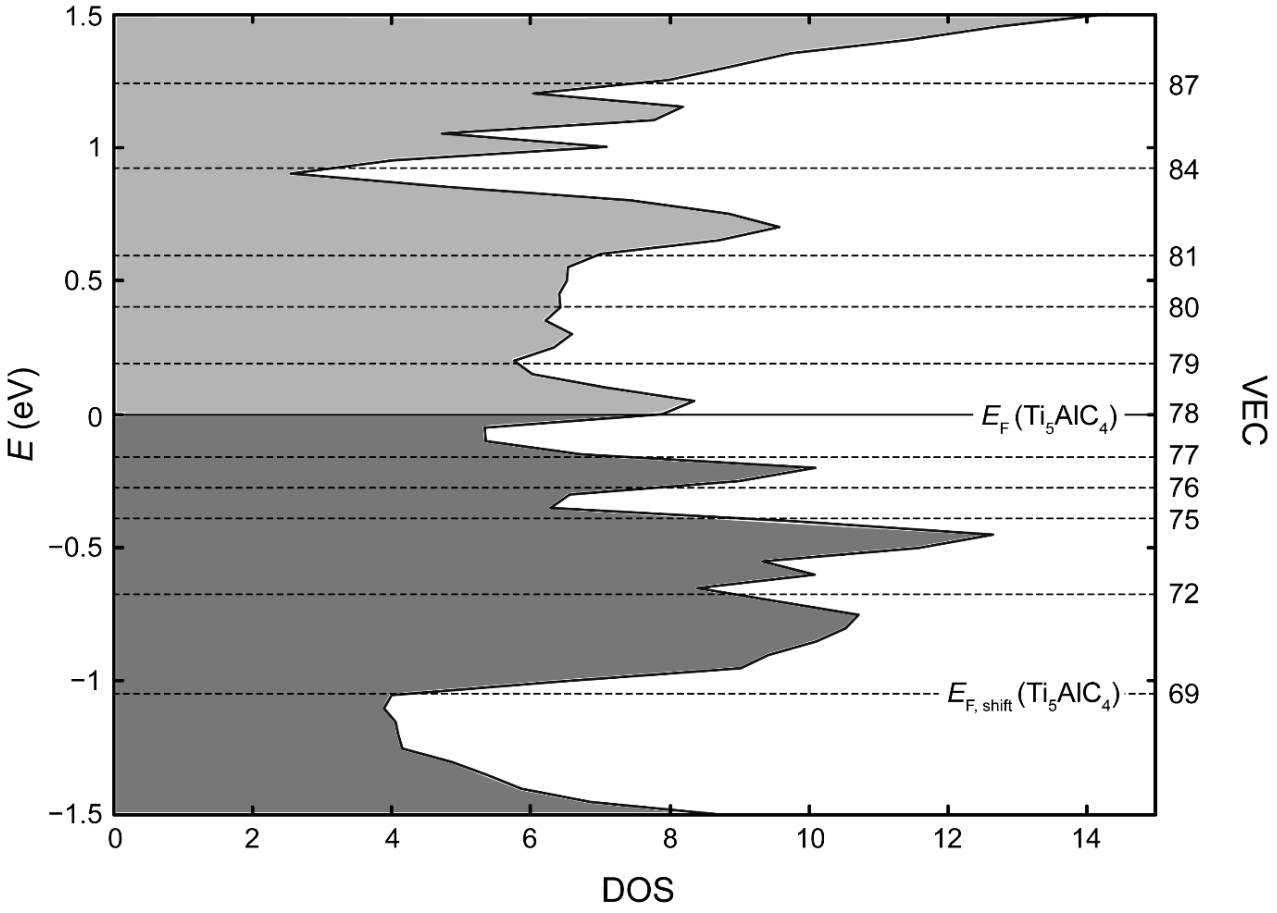

Figure 1: Total DOS plot for Ti_5CAl_4, with the solid horizontal line signifying the Fermi level E_F of the unperturbed system and the dashed lines signifying shifted Fermi levels employing the rigid-band approach, both for an excess of negative charge (states above E_F) and an excess of positive charge (states below E_F). The corresponding valence electron count (VEC) is given on the right. The lighter grayscale region signifies unoccupied states in the case of the neutral system.

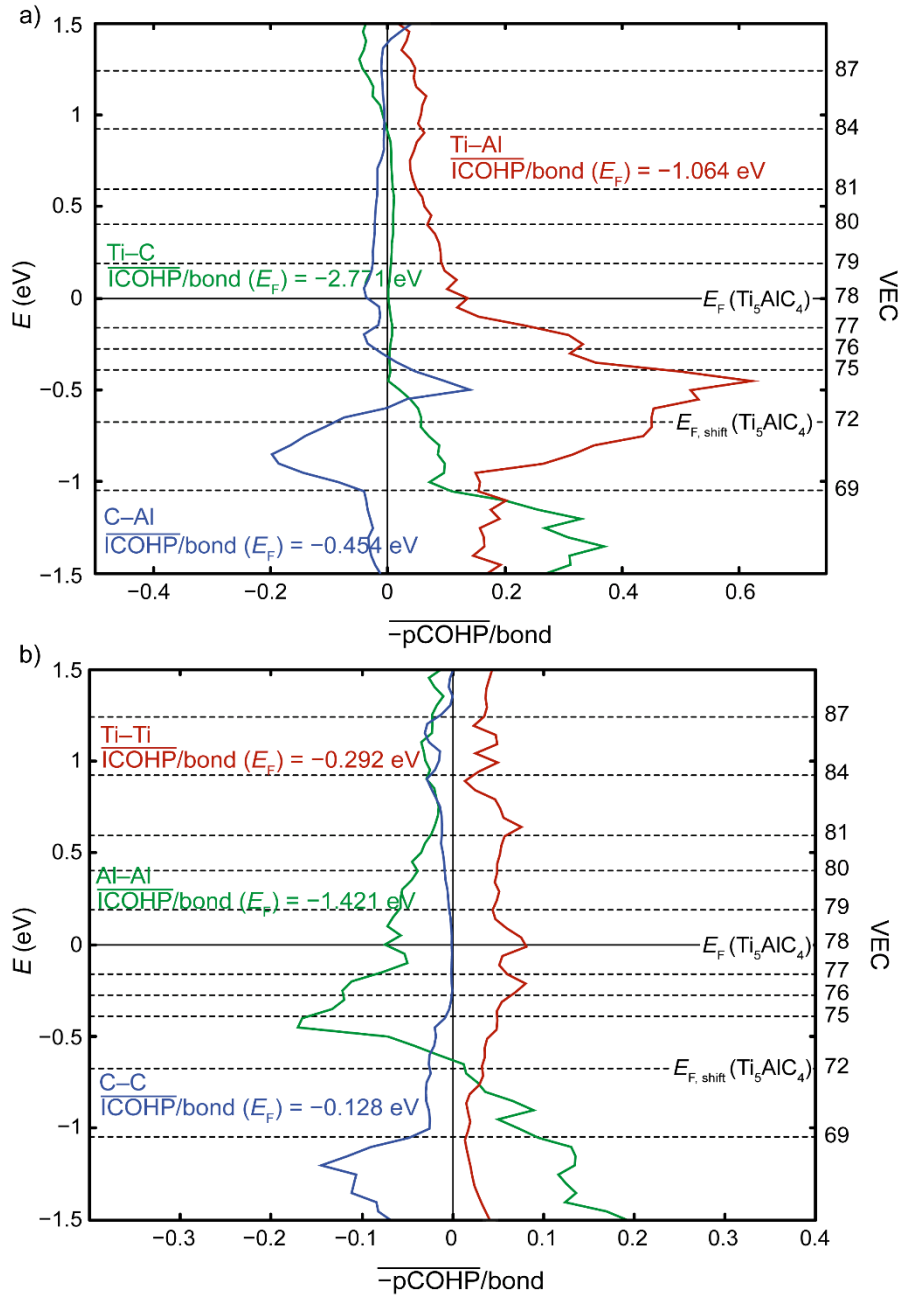

Figure 2: Energy vs. the averaged negative projected COHP per single bond for Ti_5AlC_4 using the rigid-band approach. The solid line signifies the neutral system, dashed lines signify excess negative charges (above E_F), or excess positive charges (below E_F). The corresponding valence electron count (VEC) is given on the right. a) Heteroatomic interactions: Ti–Al (red), Ti–C (green), C–Al (blue). b) Homoatomic interactions: Ti–Ti (red), Al–Al (green), C–C (blue).

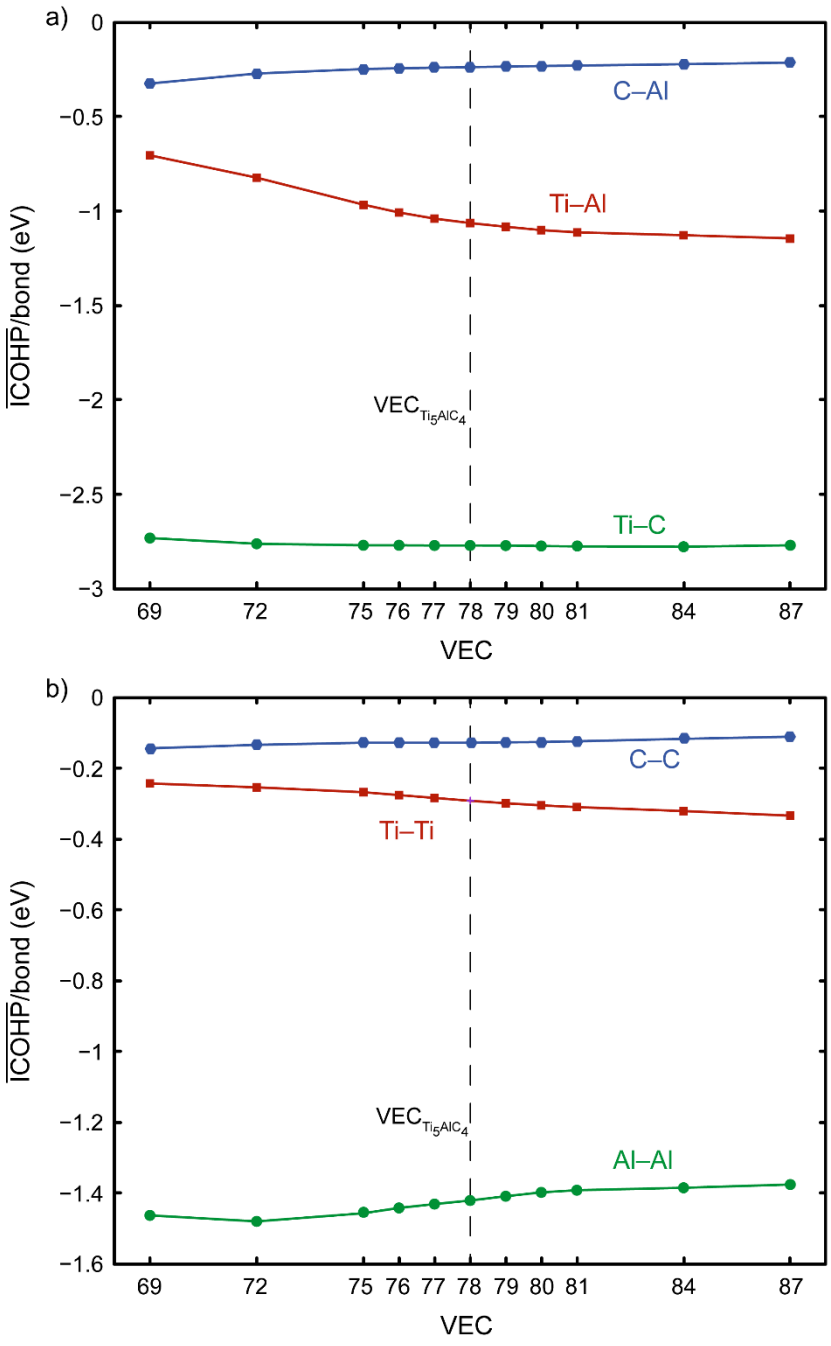

Figure 3: Averaged ICOHP per single bond as a function of the valence electron count (VEC) for Ti_5AlC_4 using the rigid-band approach. The dashed line signifies the neutral system, excess negative charges are to the right, excess positive charges to the left. a) Heteroatomic interactions: Ti–Al (red), Ti–C (green), C–Al (blue). b) Homoatomic interactions: Ti–Ti (red), Al–Al (green), C–C (blue).